by Ikoma *et al* (2009). In the striatum TACs, B_{max} values were varied from 10 to 50 pmol/mL at 5 pmol/mL intervals with other parameters fixed ($K_d = 7.9$ pmol/mL), or K_d was varied from 3 to 15 at 2 pmol/mL intervals by changing k_{on} with other parameters fixed ($B_{max} = 25.7$ pmol/mL). For each TAC, B_{max} and K_d were estimated by the MI-GA from three points obtained by MI-SRTM for the single PET scan approach and they were estimated by the graphical analysis from three points obtained by the conventional SRTM for the three PET scan approach. Then, estimates were compared with the true values. In the single PET scan approach, B_{max} and K_d were also estimated without reference TAC by the MI-GA from three points of BP_{ND} and B obtained by the two-tissue compartment four-parameter model with the plasma input function shown in the Appendix.

Analysis of Monkey Studies

PET studies were performed on three cynomolgus macaques (weight 6.9 ± 2.1 kg) with the multiple-injection approach. One animal (monN) was a healthy monkey aged 5 years, and the others had a syndrome acquired Parkinsonism. Of these, one (monUP, aged 7 years) had hemiparkinsonism induced by injecting the selective neurotoxin, *N*-methyl-4-pheny1-1,2,3,6-tetrahydropyridine (MPTP) (0.4 mg/kg) into the right carotid artery (Bankiewicz *et al*, 1986), whereas the other (monBP, aged 5 years) had bilateral Parkinsonism induced by injecting MPTP (0.4 mg/kg) intravenously and intermittently (twice a week for a total of 14 injections) (Takagi *et al*, 2005). Each Parkinsonian animal showed typical Parkinsonian symptoms in the limbs (motor slowness, tremor) unilaterally or bilaterally. The PET scan was performed after the symptom reaching stable (6 months after the first injection of MPTP). Anesthesia was induced with ketamine (8.4 mg/kg, intramuscularly) and xylazine (1.7 mg/kg, intramuscularly) and maintained by intravenous propofol (6 mg/kg/h) and vecuronium (0.02 mg/kg/h) during the scan. The monkeys were maintained and handled in accordance with guidelines for animal research on Human Care and Use of Laboratory Animals (Rockville, National Institutes of Health/Office for Protection from Research Risks, 1996). The study protocol was approved by the Subcommittee for Laboratory Animal Welfare of the National Cardiovascular Center.

After the synthesis of [^{11}C]raclopride, nonradioactive raclopride was added so that targeted molar amount of raclopride would be administered for three injections (1.5, 10, and 30 nmol/kg); this was done by dividing the [^{11}C]raclopride diluted by nonradioactive raclopride into three portions with different volumes, containing the intended masses of raclopride. For the first injection, 1.9 ± 0.16 nmol/kg (57.0 ± 5.7 MBq) of [^{11}C]raclopride was administered by a bolus injection at the beginning of the scan. Fifty minutes later, the second [^{11}C]raclopride injection, 11.1 ± 0.56 nmol/kg (60.4 ± 8.8 MBq at the time of second injection) was administered by a bolus, and 50 mins after that, a bolus of 31.1 ± 2.1 nmol/kg (30.8 ± 4.4 MBq at the time of third injection) of [^{11}C]raclopride was administered again. Data were acquired for 150 mins (10 secs × 18, 30 secs × 6, 120 secs × 7, 300 secs × 6; total 50 mins for each injection). The specific radioactivity was 4.7 ± 2.2 GBq/μmol at the time of the first injection.

PET scans were performed using a PCA-2000A positron scanner (Toshiba Medical Systems Corporation, Otawara, Japan) that provides 47 planes and a 16.2 cm axial field-of-view. The transaxial and axial spatial resolution of the PET scanner were 6.3 and 4.7 mm full width at half maximum (Herzog *et al*, 2004). A transmission scan with a 3-rod source of ^{68}Ge-^{68}Ga was performed for 20 mins for attenuation correction before the administration of [^{11}C]raclopride. Radioactivity was measured in the three-dimensional mode and the data were reconstructed by a filtered back-projection using a Gaussian filter (3 mm of full width at half maximum). Region-of-interests (ROIs) were defined manually over the left and right striatum and cerebellum for PET images, and the radioactivity concentrations in these regions were obtained. For the left and right striatum, R_1, k_2, and BP_{ND} for each injection were estimated by the MI-SRTM. In addition, parametric images were generated, estimating each parameter voxel by voxel, using the MI-SRTM with a basis function method in which the model Equation (1) was solved using linear least squares for a set of basis functions, which enables the incorporation of parameter bounds (Gunn *et al*, 1997; Ikoma *et al*, 2009). B_{max} and K_d were estimated by the MI-GA from these BP_{ND} values of left and right striatum for three injections.

In the unilateral Parkinsonian animal, three PET scans with conventional single injection with different masses of [^{11}C]raclopride were also performed for comparison with results by the multiple-injection single PET scan approach. A PET scan with a bolus injection of 2.1 nmol/kg (50.6 MBq), 11.3 nmol/kg (60.4 MBq), or 31.1 nmol/kg (30.8 MBq) of [^{11}C]raclopride was obtained on separate days. PET data were acquired for 50 mins with the same protocol as the single PET scan approach. The values of R_1, k_2, and BP_{ND} were estimated by the SRTM, and B_{max} and K_d were estimated by the conventional graphical analysis.

Results

Simulation Study

Effect of Injected Mass on BP_{ND} Estimates: In the simulations, the value of BP_{ND}, estimated by the MI-SRTM, decreased as injected molar amount of raclopride increased, that is, concentration of bound raclopride became larger. The relationship between BP_{ND} and B^{ref} had a good linear correlation to some extent; however, it did not remain linear for large B^{ref} (Figure 2A). The regression line where $B^{ref} < 20$ pmol/mL was $BP_{ND} = -0.091B^{ref} + 2.4$, $R^2 = 0.997$ for the first injection. In the relationship between BP_{ND} and B^{ref}, BP_{ND} values of the third injection were higher than those of the first injection when B^{ref} was lower than 20 pmol/mL. The ratio B^{ref}/F^{ref} was almost the same as the BP_{ND} estimated by MI-SRTM, though it was a little smaller when B^{ref} was lower than 5 pmol/mL (Figure 2B).

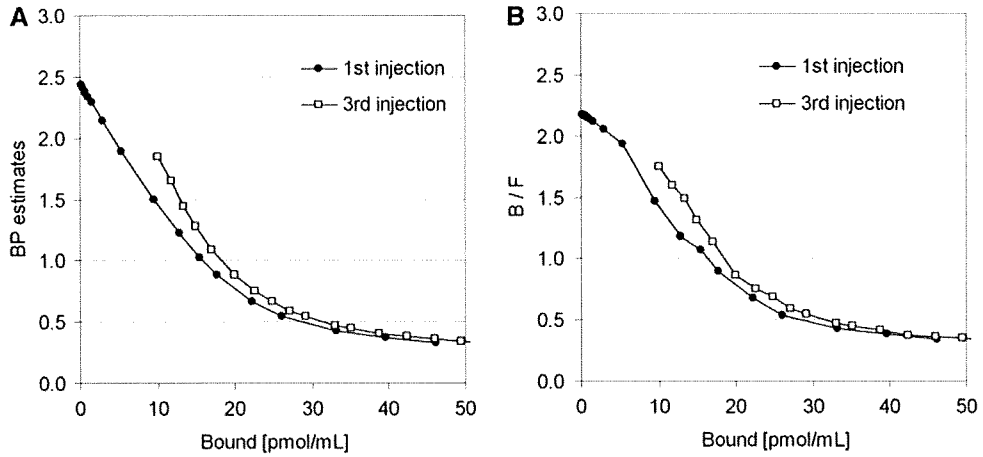

Figure 2 Relationship between specifically bound concentration and BP_{ND} (**A**) or B^{ref}/F^{ref} (**B**) estimates for the first and third injection in the simulations.

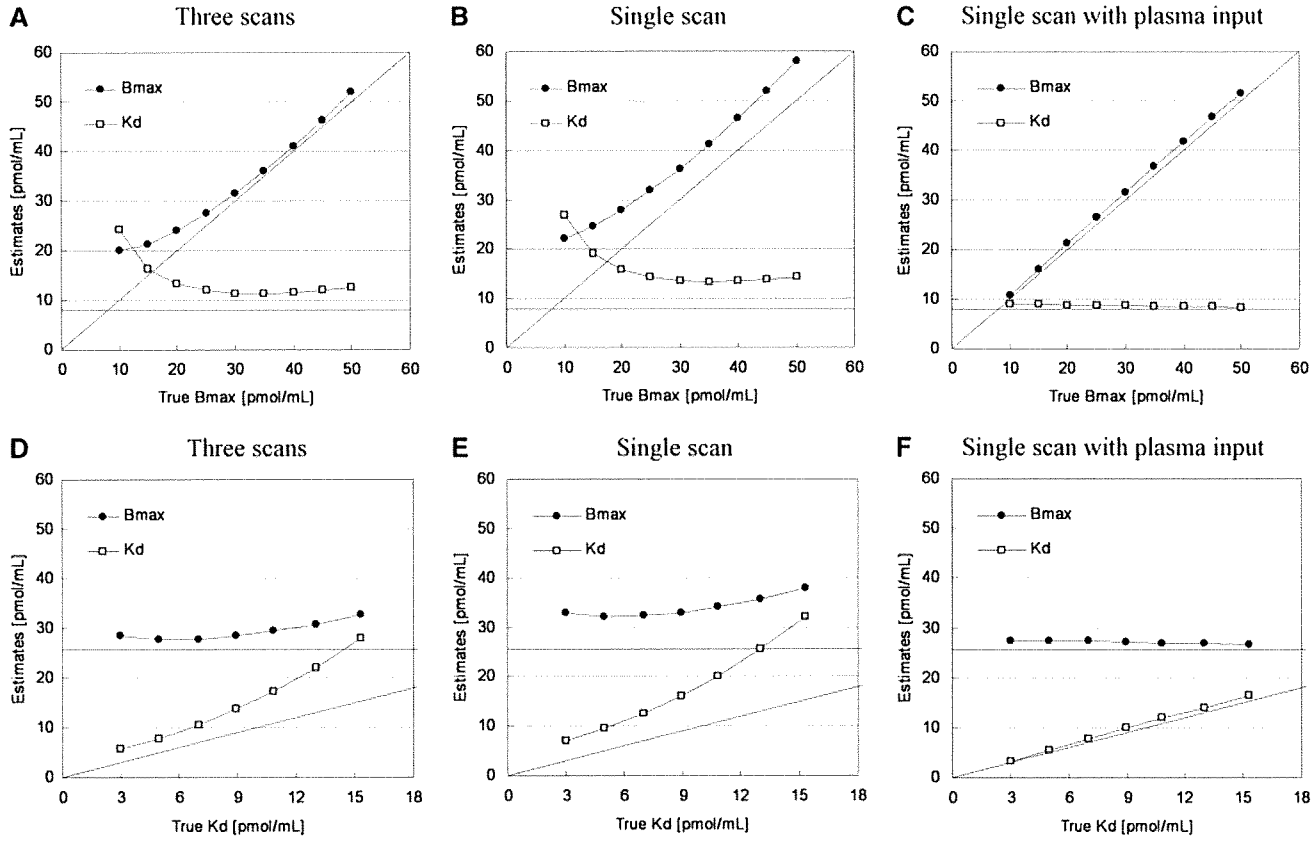

Figure 3 Relationships between estimates and true values of B_{max} and K_d for simulated TACs with various B_{max} and fixed K_d (**A**–**C**) and with various K_d and fixed B_{max} (**D**–**F**) by the three PET scan approach (**A**, **D**), multiple-injection single PET scan approach (**B**, **E**), and single PET scan approach with the plasma input function (**C**, **F**).

Estimation of B_{max} and K_d Values by the Multiple-Injection Graphical Analysis: The TACs were calculated for a range of possible B_{max} and K_d values, and the relationship between true and estimated B_{max} or K_d values was investigated for conventional three PET scan and the proposed single PET scan approaches. When B_{max} was varied, B_{max} and K_d were overestimated compared with the true values in both three PET scan and single PET scan approaches (Figures 3A and 3B). However, a good correlation was observed between true and estimated B_{max}, and there was little variation in estimated K_d when B_{max} was set higher than 20 pmol/mL. Similarly, when K_d was varied, although K_d and B_{max} were overestimated in both approaches, there was a good correlation between true and estimated K_d, and estimated B_{max} was constant (Figures 3D and 3E). In both cases, B_{max} and K_d estimates in the single

PET scan approach were higher than those in the three PET scan approach. In the TAC simulated with $B_{max} = 25.7$ and $K_d = 7.0$, estimated B_{max} and K_d were 27.8 and 10.5, respectively, in the three PET scan approach, and 32.3 and 12.6, respectively, in the single PET scan approach. In contrast to these approaches with the reference TAC, the overestimation of B_{max} and K_d was scarcely observed in the MI-GA with the plasma input function (Figures 3C and 3F).

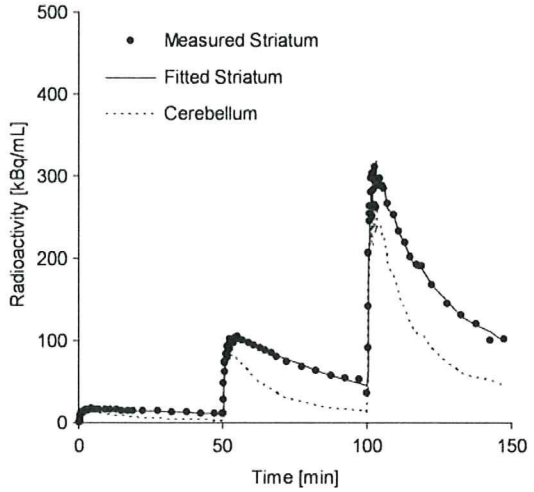

Figure 4 Measured TACs of the striatum and cerebellum and a fitted curve for the striatum using MI-SRTM in the monkey study by a single scan with sequential three injections of [^{11}C]raclopride.

Monkey Studies

Typical examples of TACs for the striatum and the cerebellum in the multiple-injection study are shown in Figure 4, and the parametric images of BP_{ND} for the first, second, and third injection, and images of B_{max} and K_d for the voxels in which BP_{ND1} was higher than 1.5 are shown in Figure 5. The estimated BP_{ND} decreased as the injected molar amount of [^{11}C]raclopride became larger in the second or third injection. Estimated BP_{ND1}, BP_{ND2}, and BP_{ND3} values were 2.3, 1.4, and 0.74, respectively, in the left striatum, and 2.6, 1.9, and 0.87, respectively, in the right striatum. The reduction in BP_{ND} was also observed in the parametric images.

The plots of MI-GA are shown in Figure 6. Plots of MI-GA for each of three animals were on the line, and B_{max} and K_d could be estimated as summarized in Table 1. Using the single scan approach for the hemiparkinsonian animal, B_{max} was 42.3 pmol/mL and K_d was 15.2 pmol/mL in the affected (right) striatum, and B_{max} was 32.3 pmol/mL and K_d was 13.0 pmol/mL in the contralateral (left) normal striatum. Corresponding estimates for the three scan approach were $B_{max} = 36.4$ and $K_d = 13.3$ pmol/mL in the right striatum and $B_{max} = 29.2$ and $K_d = 11.6$ pmol/mL in the

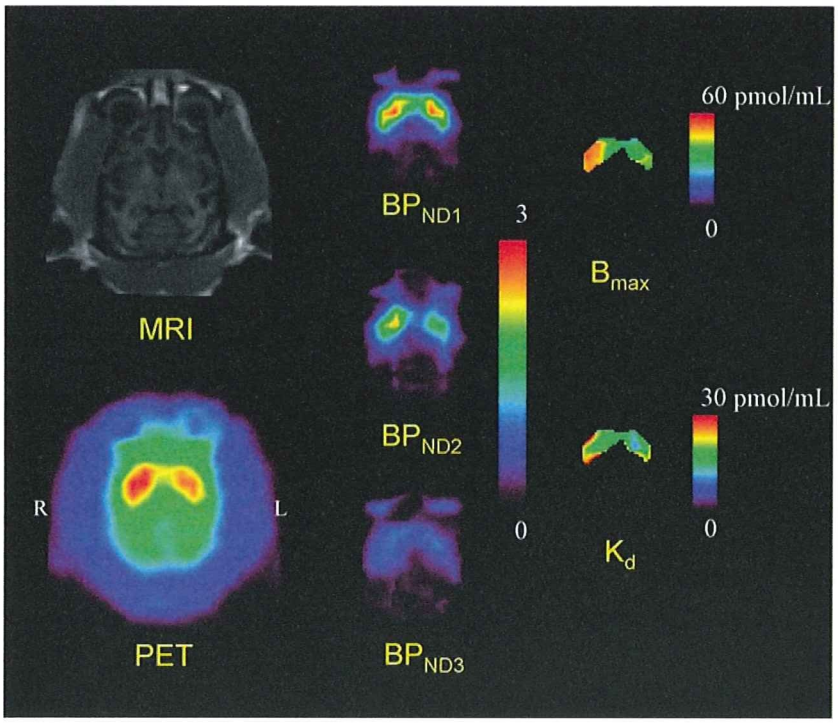

Figure 5 MRI and PET summation image (left) and parametric images of BP_{ND} for the first, second, and third injection (center) and parametric images of B_{max} and K_d for the voxels in which BP_{ND1} is higher than 1.5 (right) in the unilateral Parkinsonian (monUP) monkey study by a single scan with three sequential injections of [^{11}C]raclopride. Although ROI analysis disclosed higher B_{max} values in the MPTP-infused side of the striatum, the parametric image showed more evident increase of B_{max} in the dorsal and posterior parts of the striatum.

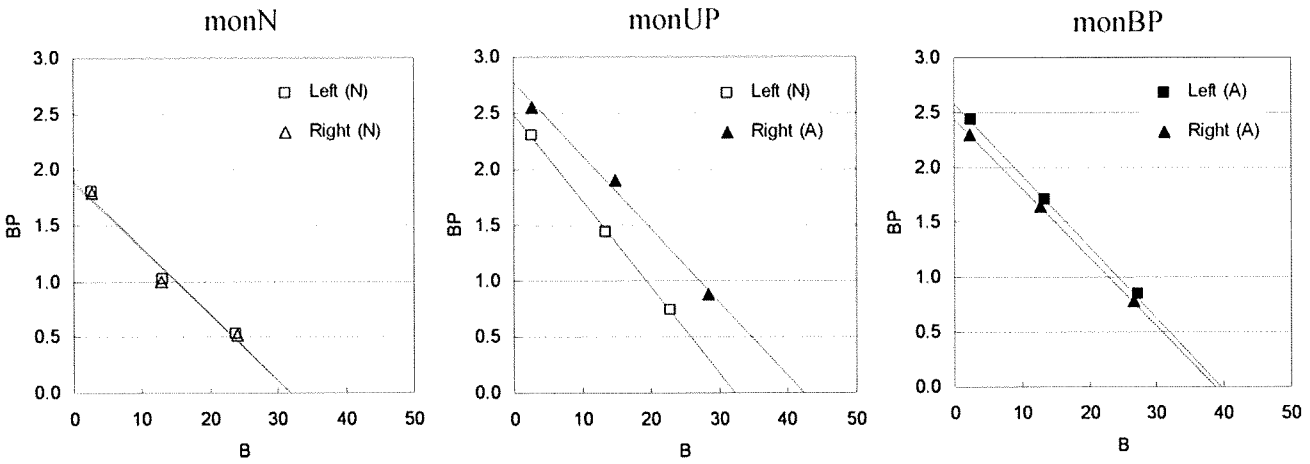

Figure 6 Single-scan, multiple-injection graphical analysis for normal (N) or affected (A) region of the left or right striatum in three monkeys that were normal (monN), unilateral Parkinsonian (monUP), and bilateral Parkinsonian (monBP).

Table 1 Estimated B_{max} and K_d values in three monkey studies

Scan protocol	*Subject*	*Region*	*Diagnosis*	B_{max} *(pmol/mL)*	K_d *(pmol/mL)*
Single scan	monN	L	N	31.8	16.7
		R	N	31.7	16.9
	monUP	L	N	32.3	13.0
		R	A	42.3	15.2
	monBP	L	A	39.6	15.4
		R	A	38.7	15.9
Three scans	monUP	L	N	29.2	11.6
		R	A	36.4	13.3

L, left striatum; R, right striatum; N, normal striatum; A, affected striatum.

left striatum. Both B_{max} and K_d of the single PET scan approach were slightly higher than those of the three PET scan approach. However, importantly, both approaches found that B_{max} in the affected striatum was higher than that in the normal striatum. The bilateral Parkinsonian animal showed B_{max} values of left = 39.6 pmol/mL, right = 38.7 pmol/mL, both of which were higher than those of the striatum of the normal animal or the normal striatum of the unilateral animal, but were very close to the affected striatum of the unilateral animal. The K_d values of the bilateral animal were not so different from other striatums.

Discussion

Density and Affinity Determination by Graphical Analysis with the Reference Region

In the graphical analysis for PET receptor studies, the values of B_{max} and K_d were estimated from the relationship between the ratio of bound to free concentrations and bound concentration at the time of transient equilibrium, using the TAC of the reference region (Farde *et al*, 1986). Some groups have used the value estimated from the distribution volume ratio − 1, instead of the B^{ref}/F^{ref} value of the y axis, because the values of B^{ref}/F^{ref} could change considerably with small changes in the time point of the transient equilibrium T_{eq} determined as the maximum C_b^{ref} (Logan *et al*, 1997; Doudet and Holden, 2003; Doudet *et al*, 2003). Distribution volume ratio or BP_{ND} is estimated from the kinetic analysis with TACs of target and reference regions, so it is not affected by the error of estimated T_{eq}. On the other hand, the value of $k'_3(t)$ in Equation (2) varies according to the concentration of bound raclopride, and estimates of BP_{ND} are considered to be an averaged value of specific binding over time, which is influenced by the dynamics of the free and bound raclopride. Despite this, in our simulation study of [^{11}C]raclopride, there was little difference between B^{ref}/F^{ref} and BP_{ND} estimated by the SRTM, and both had a linear correlation with B^{ref} (Figure 2). However, B^{ref}/F^{ref} became smaller than BP_{ND} and deviated from the linear relationship between B^{ref}/F^{ref} and B^{ref} in the region with low B^{ref} (Figure 2), especially for the TACs with high B_{max}. This may be a result of imperfect attainment of the transient equilibrium within the 50 mins scan duration for the TAC with high binding. There was little effect of the error of B^{ref} for the graphical analysis, in which B^{ref} varied widely among three injections, whereas the error of B^{ref}/F^{ref}

because of nonachievement of transient equilibrium had much effect on the graphical analysis as compared with BP_{ND}. Therefore, we estimated B_{max} and K_d by the graphical analysis with the relationship between BP_{ND} and B^{ref}.

In the simulations with various injected masses of [^{11}C]raclopride, it was shown that the relationship between BP_{ND} and B^{ref} became linear to some extent. However, BP_{ND} deviated from the linear relationship and approached a nonzero value when B^{ref} became larger (Figure 2). Therefore, in the B_{max} and K_d estimation by the graphical analysis with the reference TAC, points must be plotted within the range of the linear relation. As the relationship between BP_{ND} and B estimated from C_b using the plasma input function, without the reference TAC, remained linear even when B became large and the estimated BP_{ND} approached 0 (data not shown), this apparent saturation seemed to be owing to the reference region. Strictly speaking, the time course of free radioligand C_f is different from that of the reference region C_r (Figure 1) and C_f changes according to the specific binding that was affected by k_{on}, B_{max}, or administered mass of raclopride as pointed out by Ito *et al* (1998). Therefore, the time of the transient equilibrium estimated using C_b^{ref} was different from that estimated using C_b, and B^{ref} was often different as well. In addition, the value of BP_{ND} estimated by SRTM was lower than the BP_{ND} estimated from the two-tissue compartment model with the plasma input function.

This difference between the target and reference TAC affected the B_{max} and K_d estimates as well. In the simulated TACs with various B_{max} or K_d values, the B_{max} and K_d were overestimated compared with the true values even in the conventional three PET scan approach (Figure 3). On the other hand, the overestimation was not observed when B_{max} and K_d were estimated by the graphical analysis using C_f and C_b without the reference TAC (Figure 3), demonstrating that graphical analysis could determine B_{max} and K_d precisely if C_b were obtained correctly. However, the free and bound concentrations in the target region cannot be distinguished from the total concentration measured by PET scanning without arterial blood sampling, and in practical PET data, estimation of rate constants with the plasma input function is unstable and impractical. Therefore, in the usual graphical analysis, the TAC of reference region is used as the free radioligand concentration in the target region (Farde *et al*, 1989). The effect of the reference TAC on B_{max} and K_d estimates depends on the kinetics of the tracer in each region, which depends in turn on the particular tracers and species. In the simulated TACs of monkeys with [^{11}C]raclopride, there was a good correlation between true and estimated K_d or B_{max}, though estimates were biased. Therefore, we concluded the graphical analysis with reference TAC is practical for [^{11}C]raclopride studies, because it can detect the value of B_{max} or K_d in neurological or psychiatric disorders without arterial blood sampling.

Estimated Density and Affinity by the Multiple-Injection Approach

We applied the multiple-injection approach to the graphical analysis for B_{max} and K_d determination in an effort to shorten the total duration of the scanning protocol, and to obviate the need for several radiosyntheses for each animal. From the relationship between the BP_{ND} estimates and injected mass in the simulation study (Figure 2), the molar amounts of three injections were set as 1.5, 10, and 30 nmol/kg, so that the estimated BP_{ND} would be high, intermediate, and low within the range in which the linear correlation held. The injection interval was set to 50 mins, because it has been reported in monkey studies that 50 mins scan duration could provide reliable BP_{ND} estimates even for TACs with high and low BP_{ND} values (Ikoma *et al*, 2009). In our present studies on monkeys with this protocol, injected masses increased with each successive injection, but amounts of administered radioactivity remained fairly constant, i.e., 57, 60, and 31 MBq. Therefore, the signal to noise ratio of image quality did not change seriously for each injection.

In the usual graphical analysis by nonsequential multiple PET scans, the molar amount of administered [^{11}C]raclopride for each scan is adjusted by varying the specific activity of administered [^{11}C]raclopride. Several investigators have attempted to perform multiple injections of ligands with PET studies to obtain receptor density and affinity by changing specific activity with a detailed model equation (Delforge *et al*, 1995; Millet *et al*, 1995; Morris *et al*, 1996; Muzic *et al*, 1996; Christian *et al*, 2004; Gallezot *et al*, 2008). Meanwhile, our approach requires only one synthesis of [^{11}C]raclopride, which is split to three with different mass of raclopride with same specific activity. By keeping the specific activity throughout scan, we can directly interpret PET counts in pmol/mL unit.

In the simulations of B_{max} and K_d estimation with this single PET scan approach, B_{max} and K_d were overestimated compared with the true values, just as seen in the three PET scan approach. Furthermore, estimates of both parameters were higher than those in the three PET scan approach. In the single PET scan approach, the error because of assumptions of the reference tissue approach could be more severe than for the three PET scan approach, because the residual radioactivities at the times of the second and third injections could propagate to error of B^{ref} or BP_{ND} estimates. This was shown to be the case in the simulation study, in which the relationship between the BP_{ND} and B^{ref} in the third injection was a little different from that in the first injection (Figure 2). Furthermore, our approach assumes that BP_{ND} is promptly altered by the next injection, but this is in fact not exactly the case. We showed the bias of the estimated BP_{ND} related to this assumption (Ikoma *et al*, 2009), and the estimated B_{max} and K_d in this paper consequently could be biased. However, in the

simulations, B_{max} and K_d estimated by the MI-GA changed according to the variation of the true values (Figure 3), demonstrating this approach could be applied to the quantitative evaluation of B_{max} and K_d from a single session of PET scanning.

Monkey Studies

In the simulations, we demonstrated that the MI-GA could detect density and affinity of dopamine D_2 receptors. Furthermore, we demonstrated the validity of the proposed method using actual data from monkeys. As a result, the three BP_{ND} data points calculated from the single PET scan with three sequential injections of different administration masses were almost on a straight line, and estimated values of B_{max} and K_d were very close to those previously obtained *in vitro* ($B_{max} = 25.7$ pmol/g) (Madras *et al*, 1988) or *in vivo* by the conventional method in monkeys ($B_{max} = 22$ pmol/mL, $K_d = 13.5$ nmol/L) (Doudet *et al*, 2003). The estimates by the single PET scan approach were slightly higher than those by the three PET scan approach, and this was consistent with the results from the current simulations.

Although we investigated only three monkeys in this study, the values of B_{max} in the partially denervated striata was higher than in normal striatum, whereas the apparent affinity was unaffected by the MPTP lesions. Likewise Rinne *et al* (1995) reported a 35% increase in the D_2 B_{max} in the putamen contralateral to the side of predominant motor symptoms, without any discernible effect on apparent affinity. In our monkey measurements, in the hemilesioned monkey, the B_{max} was elevated by 31% on the denervated side. In the animal with bilateral MPTP lesion, the B_{max} in both striata was higher than in the normal animal, or in the unlesioned side of the hemiparkinsonian animal, despite no significant changes in K_d values: the results were consistent with those of the previous report.

In addition to the results of ROI analysis, which disclosed bulk D_2 receptor characteristics in the whole striatum, parametric imaging of B_{max} and K_d (as shown in Figure 5) suggested a potential significance in regional estimation of D_2 receptor characteristics. Although ROI analysis disclosed higher B_{max} values in the MPTP-infused side of the striatum, the parametric imaging showed the increase of B_{max} was more evident in the dorsal and posterior parts of the striatum. A similar finding of preferential lesion in dorsal and posterior parts of the striatum has been reported based on neurochemical and pathological assessments of MPTP-lesioned monkeys (Oiwa *et al*, 2003). As the current parametric imaging may have significant artifacts, such as those arising from low signal-to-noise ratio, partial volume effects, small number of points, the situation should be improved through the use of a higher resolution PET scanner.

Potential Limitations of the Multiple-Injection Graphical Analysis

The multiple-injection approach is able to assess the B_{max} and K_d for receptor studies in a single PET scan with single radiosynthesis, and shortened study period as compared with a conventional approach. This approach might also be applicable to other PET ligands and receptor types, but with several caveats: First, it is necessary to evaluate whether the reference region can be used as the free TAC of the target region. The kinetics of the target and reference regions is affected by the value of each rate constant, i.e., K_1, k_2, B_{max}, and K_d, that differ between species and radioligands. The difference between C_{ref} and C_f often causes an error in B^{ref}, and the estimated B_{max} and K_d should be interpreted with caution when the reference region has considerably different kinetics. Second, the molar amounts of administered ligand need to be selected such that the resultant BP_{ND} will be within the range in which the linear relationship between BP_{ND} and B holds. In the case of regions with low BP_{ND}, and small extent of the necessary linear relationship, it may be difficult to determine B_{max} and K_d reliably. Third, the interval of three injections should be determined so that the free ligand TAC has a transient equilibrium within the scan duration of each injection, especially when the injected mass is small, i.e., BP_{ND} is high. The radioligand [^{11}C]raclopride dissociates rapidly from the receptors, allowing equilibration of binding to be established *in vivo* within the time span of PET experiments (Farde *et al*, 1989; Ito *et al*, 1998). However, those ligands with slow kinetics, such as [^{18}F]fallypride require a longer scan duration such that the present graphical analysis may not be suitable in all instances. Despite these limitations, by optimizing the administered mass and the time interval between three injections of [^{11}C]raclopride, we have shown that the multiple-injection approach can determine B_{max} and K_d values as effectively as an approach using three separate scans, but within a single scan time of 150 mins.

Moreover, the bias of B_{max} and K_d estimated by the single scan approach with two injections was not larger than that by the single scan approach with three injections in the simulations (data not shown), and points of the second and third injections in MI-GA were almost on the same line in the monkey studies (Figure 6). Therefore, there is a possibility of reducing scan time and exposure further using only two injections, though the effect of statistical noise on estimates should be considered.

Conclusion

We developed the method for estimating B_{max} and K_d values in a single session of PET scanning with multiple injections of [^{11}C]raclopride. Our simulations showed that the MI-GA could detect B_{max} and K_d values by using the optimal injection protocol. We

also demonstrated in monkey studies that B_{max} and K_d values estimated by our proposed approach were proper compared with previous monkey studies or our studies by the conventional method. The proposed method made it possible to determine the dopamine D_2 receptor density and affinity by a 150 mins PET scan with three injections of [^{11}C]raclopride at 50 mins intervals.

Acknowledgements

We thank Dr Jun Takahashi (Kyoto University) for providing us animals for this study. This research was supported by the Ministry of Education, Culture, Sports, Science and Technology of Japan (MEXT) grant-in-aid for Young Scientists (B) (No. 20790839), grant-in-aid for Scientific Research (C) (No. 09019855) (TH), Kobe Cluster I and II, and the Ministry of Health, Labour, and Welfare of Japan (MHLW) Health Science Research Grant, H17-025 (TH, HI). We are grateful to members of Department of Investigative Radiology, National Cardiovascular Center Research Institute, for their support of PET experiment and for helpful suggestions.

Conflict of interest

The authors declare no conflict of interest.

References

Bankiewicz KS, Oldfield EH, Chiueh CC, Doppman JL, Jacobowitz DM, Kopin IJ (1986) Hemiparkinsonism in monkeys after unilateral internal carotid artery infusion of 1-methyl-4-phenyl-1,2,3,6-tetrahydropyridine (MPTP). *Life Sci* 39:7–16

Christian BT, Narayanan T, Shi B, Morris ED, Mantil J, Mukherjee J (2004) Measuring the *in vivo* binding parameters of [^{18}F]-fallypride in monkeys using a PET multiple-injection protocol. *J Cereb Blood Flow Metab* 24:309–22

Cross AJ, Crow TJ, Owen F (1981) ^{3}H-Flupenthixol binding in post-mortem brains of schizophrenics: evidence for a selective increase in dopamine D2 receptors. *Psychopharmacology (Berl)* 74:122–4

Delforge J, Pappata S, Millet P, Samson Y, Bendriem B, Jobert A, Crouzel C, Syrota A (1995) Quantification of benzodiazepine receptors in human brain using PET, [^{11}C]flumazenil, and a single-experiment protocol. *J Cereb Blood Flow Metab* 15:284–300

Doudet DJ, Holden JE (2003) Sequential versus non-sequential measurement of density and affinity of dopamine D_2 receptors with [^{11}C]raclopride: Effect of methamphetamine. *J Cereb Blood Flow Metab* 23:1489–94

Doudet DJ, Jivan S, Holden JE (2003) *In vivo* measurement of receptor density and affinity: comparison of the routine sequential method with a nonsequential method in studies of dopamine D_2 receptors with [^{11}C]raclopride. *J Cereb Blood Flow Metab* 23:280–4

Farde L, Ehrin E, Eriksson L, Greitz T, Hall H, Hedström CG, Litton JE, Sedvall G (1985) Substituted benzamides as ligands for visualization of dopamine receptor binding in the human brain by positron emission tomography. *Proc Natl Acad Sci USA* 82:3863–7

Farde L, Eriksson L, Blomquist G, Halldin C (1989) Kinetic analysis of central [^{11}C]raclopride binding to D_2-dopamine receptors studied by PET — A comparison to equilibrium analysis. *J Cereb Blood Flow Metab* 9: 696–708

Farde L, Hall H, Ehrin E, Sedvall G (1986) Quantitative analysis of D_2 dopamine receptor binding in the living human brain by PET. *Science* 231:258–61

Farde L, Wiesel FA, Hall H, Halldin C, Stone-Elander S, Sedvall G (1987) No D_2 receptor increase in PET study of schizophrenia. *Arch Gen Psychiatry* 44:671–2

Farde L, Wiesel FA, Stone-Elander S, Halldin C, Nordström AL, Hall H, Sedvall G (1990) D_2 dopamine receptors in neuroleptic-naive schizophrenic patients. A positron emission tomography study with [^{11}C]raclopride. *Arch Gen Psychiatry* 47:213–9

Gallezot JD, Bottlaender MA, Delforge J, Valette H, Saba W, Dollé F, Coulon CM, Ottaviani MP, Hinnen F, Syrota A, Grégoire MC (2008) Quantification of cerebral nicotinic acetylcholine receptors by PET using 2-[^{18}F]fluoro-A-85380 and the multiinjection approach. *J Cereb Blood Flow Metab* 28:172–89

Gunn RN, Lammertsma AA, Hume SP, Cunningham VJ (1997) Parametric imaging of ligand-receptor binding in PET using a simplified reference region model. *Neuroimage* 6:279–87

Guttman M, Seeman P (1985) L-dopa reverses the elevated density of D_2 dopamine receptors in Parkinson's diseased striatum. *J Neural Transm* 64:93–103

Hall H, Köhler C, Gawell L, Farde L, Sedvall G (1988) Raclopride, a new selective ligand for the dopamine-D_2 receptors. *Prog Neuropsychopharmacol Biol Psychiatry* 12:559–68

Herzog H, Tellmann L, Hocke C, Pietrzyk U, Casey ME, Kuwert T (2004) NEMA NU2-2001 guided performance evaluation of four Siemens ECAT PET scanners. *IEEE Trans Nucl Science* 51:2662–9

Ikoma Y, Watabe H, Hayashi T, Miyake Y, Teramoto N, Minato K, Iida H (2009) Quantitative evaluation of changes in binding potential with a simplified reference tissue model and multiple injections of [^{11}C]raclopride. *Neuroimage* 47:1639–48

Ito H, Hietala J, Blomqvist G, Halldin C, Farde L (1998) Comparison of the transient equilibrium and continuous infusion method for quantitative PET analysis of [^{11}C]raclopride binding. *J Cereb Blood Flow Metab* 18:941–50

Joyce JN, Lexow N, Bird E, Winokur A (1988) Organization of dopamine D_1 and D_2 receptors in human striatum: receptor autoradiographic studies in Huntington's disease and schizophrenia. *Synapse* 2:546–57

Köhler C, Hall H, Ogren SO, Gawell L (1985) Specific *in vitro* and *in vivo* binding of ^{3}H-raclopride. A potent substituted benzamide drug with high affinity for dopamine D-2 receptors in the rat brain. *Biochem Pharmacol* 34:2251–9

Lammertsma AA, Hume SP (1996) Simplified reference tissue model for PET receptor studies. *Neuroimage* 4:153–8

Logan J, Fowler JS, Volkow ND, Wang GJ, Ding YS, Alexoff DL (1996) Distribution volume ratios without blood sampling from graphical analysis of PET data. *J Cereb Blood Flow Metab* 16:834–40

Logan J, Volkow ND, Fowler JS, Wang GJ, Fischman MW, Foltin RW, Abumard NN, Vitkun S, Gatley SJ, Pappas N, Hitzemann R, Shea CE (1997) Concentration and occupancy of dopamine transporters in cocaine abusers with [^{11}C]cocaine and PET. *Synapse* 27:347–56

Madras BK, Fahey MA, Canfield DR, Spealman RD (1988) D1 and D2 dopamine receptors in caudate-putamen of nonhuman primates (*macaca fascicularis*). *J Neurochem* 51:934–43

Millet P, Delforge J, Mauguiere F, Pappata S, Cinotti L, Frouin V, Samson Y, Bendriem B, Syrota A (1995) Parameter and index images of benzodiazepine receptor concentration in the brain. *J Nucl Med* 36:1462–71

Mintun MA, Raichle ME, Kilbourn MR, Wooten GF, Welch MJ (1984) A Quantitative model for the *in vivo* assessment of drug binding sites with positron emission tomography. *Ann Neurol* 15:217–27

Morris ED, Babich JW, Alpert NM, Bonab AA, Livni E, Weise S, Hsu H, Christian BT, Madras BK, Fischman AJ (1996) Quantification of dopamine transporter density in monkeys by dynamic PET imaging of multiple injections of ^{11}C-CFT. *Synapse* 24:262–72

Muzic RR, Nelson AD, Saidel GM, Miraldi F (1996) Optimal experiment design for PET quantification of receptor concentration. *IEEE Trans Med Imaging* 15:2–12

Oiwa Y, Eberling JL, Nagy D, Pivirotto P, Emborg ME, Bankiewicz KS (2003) Overlesioned hemiparkinsonian non human primate model: correlation between clinical, neurochemical and histochemical changes. *Front Biosci* 8:155–66

Rinne JO, Laihinen A, Ruottinen H, Ruotsalainen U, Någren K, Lehikoinen P, Oikonen V, Rinne UK (1995) Increased density of dopamine D_2 receptors in the putamen, but not in the caudate nucleus in early Parkinson's disease: a PET study with [^{11}C]raclopride. *J Neurol Sci* 132:156–61

Scatchard G (1949) The attractions of proteins for small molecules and ions. *Ann NY Acad Sci* 51:660–72

Seeman P, Bzowej NH, Guan HC, Bergeron C, Reynolds GP, Bird ED, Riederer P, Jellinger K, Tourtellotte WW (1987) Human brain D_1 and D_2 dopamine receptors in schizophrenia, Alzheimer's, Parkinson's, and Huntington's diseases. *Neuropsychopharmacology* 1:5–15

Takagi Y, Takahashi J, Saiki H, Morizane A, Hayashi T, Kishi Y, Fukuda H, Okamoto Y, Koyanagi M, Ideguchi M, Hayashi H, Imazato T, Kawasaki H, Suemori H, Omachi S, Iida H, Itoh N, Nakatsuji N, Sasai Y, Hashimoto N (2005) Dopaminergic neurons generated from monkey embryonic stem cells function in a Parkinson primate model. *J Clin Invest* 115:102–9

Watabe H, Ohta Y, Teramoto N, Miyake Y, Kurokawa M, Yamamoto A, Ose Y, Hayashi T, Iida H (2006) A novel reference tissue approach for multiple injections of [C-11]Raclopride. *Neuroimage* 31:T73

Wong DF, Wagner Jr HN, Tune LE, Dannals RF, Pearlson GD, Links JM, Tamminga CA, Broussolle EP, Ravert HT, Wilson AA, Toung JK, Malat J, Williams JA, O'Tuama LA, Snyder SH, Kuhar MJ, Gjedde A (1986) Positron emission tomography reveals elevated D_2 dopamine receptors in drug-naive schizophrenics. *Science* 234:1558–63

Appendix

The multiple-injection two-tissue four-parameter compartment model is based on the following differential equations:

$$\frac{dC_f}{dt} = K_1 C_p(t) - (k_2 + k_3) C_f(t) + k_4 C_b(t) \qquad \text{(A1)}$$

$$\frac{dC_b}{dt} = k_3 C_f(t) - k_4 C_b(t) \qquad \text{(A2)}$$

where C_p is the radioactivity concentration of metabolite-corrected plasma, C_f and C_b are the concentrations of radioactivity for free and specifically bound ligand in tissue, respectively.

Equations (A1) and (A2) are solved with the radioactivity concentration of C_f and C_b at the time of injection, that is $C_f(0)$ and $C_b(0)$, then $C_f(t)$, $C_b(t)$ and total radioactivity concentration in tissue $C_t(t)$ are expressed as following equations:

$$\begin{aligned} C_f(t) = {} & \frac{K_1}{\alpha_2 - \alpha_1}\{(k_4 - \alpha_1)e^{-\alpha_1 t} - (k_4 - \alpha_2)e^{-\alpha_2 t}\} \otimes C_p(t) \\ & + \frac{1}{\alpha_2 - \alpha_1}\{(k_4 - \alpha_1)C_f(0) + k_4 C_b(0)\}e^{-\alpha_1 t} \\ & - \frac{1}{\alpha_2 - \alpha_1}\{(k_4 - \alpha_2)C_f(0) + k_4 C_b(0)\}e^{-\alpha_2 t} \end{aligned} \qquad \text{(A3)}$$

$$\begin{aligned} C_b(t) = {} & \frac{K_1 k_3}{\alpha_2 - \alpha_1}\left(e^{-\alpha_1 t} - e^{-\alpha_2 t}\right) \\ & \otimes C_p(t) + \frac{k_3}{\alpha_2 - \alpha_1}\left(C_f(0) + \frac{k_4}{k_4 - \alpha_1} C_b(0)\right)e^{-\alpha_1 t} \\ & - \frac{k_3}{\alpha_2 - \alpha_1}\left(C_f(0) + \frac{k_4}{k_4 - \alpha_2} C_b(0)\right)e^{-\alpha_2 t} \\ & + \left(\frac{k_3 k_4}{(k_4 - \alpha_1)(k_4 - \alpha_2)} + 1\right) C_b(0) e^{-k_4 t} \end{aligned} \qquad \text{(A4)}$$

$$\begin{aligned} C_t(t) = {} & \frac{K_1}{\alpha_2 - \alpha_1}\{(k_3 + k_4 - \alpha_1)e^{-\alpha_1 t} - (k_3 + k_4 - \alpha_2)e^{-\alpha_2 t}\} \\ & \otimes C_p(t) + \frac{k_3 + k_4 - \alpha_1}{\alpha_2 - \alpha_1}\left(C_f(0) + \frac{k_4}{k_4 - \alpha_1} C_b(0)\right)e^{-\alpha_1 t} \\ & - \frac{k_3 + k_4 - \alpha_2}{\alpha_2 - \alpha_1}\left(C_f(0) + \frac{k_4}{k_4 - \alpha_2} C_b(0)\right)e^{-\alpha_2 t} \\ & + \left(\frac{k_3 k_4}{(k_4 - \alpha_1)(k_4 - \alpha_2)} + 1\right) C_b(0) e^{-k_4 t} \\ \alpha_{1,2} = {} & \frac{(k_2 + k_3 + k_4) \mp \sqrt{(k_2 + k_3 + k_4)^2 - 4k_2 k_4}}{2} \end{aligned} \qquad \text{(A5)}$$

薬理学・毒性学

GSK-3βと創薬

GSK-3β and drug development

グリコーゲン合成酵素キナーゼ(GSK)-3βは，糖をグリコーゲンとして貯蔵させる酵素をリン酸化により抑制する酵素として見出された．GSK-3βはインスリンにより活性が抑制されることが知られていたが，今日，インスリンのほかにも種々のシグナルを受け，増殖や分化など基本的な生体反応に関与することがわかっている．

GSK-3βが属するGSK-3ファミリーには他に2種(αとβ2)がある．αとβの相同性は高いが，β欠損は致死的なので代償性は限られると考えられる．β2はスプライシングが異なるが，機能的な差異は不明である．GSK-3βの制御様式は多様で，①種々の蛋白分子との結合，②リン酸化(Ser^9リン酸化による抑制，Tyr^{216}リン酸化による活性化)，③プライミング(基質はリン酸化部位近傍のSerが他のキナーゼによりあらかじめリン酸化される必要がある)のほか，④細胞内局在の変化も示唆される．

GSK-3β阻害薬

躁病(双極性障害)へのリチウムの効果は1948年に見出され，1954年のプラセボ対照試験で証明されたが，機序は不明であった．1990年代半ば，リチウムがGSK-3βを阻害することが示され，今日ではこれが双極性障害への薬効のおもな機序と考えられている．つまりGSK-3βは古くから治療薬の標的になっていたわけだが，GSK-3βの多彩な機能が明らかになるにつれ，双極性障害以外にも種々の疾患でGSK-3β阻害が有効ではないかと考えられ，数多くの阻害薬が合成されている[1]．

双極性障害以外の精神神経疾患で，もっとも注目されてきたのはAlzheimer病(AD)であろう．家族性ADの細胞ではAkt活性の低下とともにGSK-3β活性が上昇していること，ADの特徴のひとつである微小管結合蛋白Tauの過リン酸化にGSK-3βが関与することなどがわかっているため，GSK-3β阻害薬はADの進行を抑える可能性があると考えられている．そのほか，パーキンソン病や脳梗塞などでも，GSK-3β阻害薬は神経細胞を保護すると期待されている．

また，GSK-3β阻害薬はグリコーゲン合成酵素の抑制を解除してインスリン感受性を高めるため，2型糖尿病の治療薬になる可能性がある．種々の培養細胞で，リチウムその他の阻害薬がインスリン作用に類似したブドウ糖取込み促進，グリコーゲン合成促進，糖新生抑制をもたらす[2]．

GSK-3β刺激薬

GSK-3βは，Wnt/β-カテニン情報伝達系の主要構成因子でもある．

Wnt/β-カテニン系の活性は，細胞質β-カテニン量で決定される．β-カテニンはGSK-3βでリン酸化されるとユビキチン化されて分解され，通常低レベルに抑えられている．Wnt刺激がGSK-3βを阻害すると，β-カテニンが集積して核へ移行し，転写因子TCFと複合体をつくり，数多くの遺伝子の転写を促す．

Wnt/β-カテニン系構成因子の変異が多くの癌でみつかり，また，この系の標的遺伝子にはc-mycやサイクリンD1など細胞増殖の主要調節因子も含まれるため，GSK-3βなど，この系の因子を標的にすれば，新規抗癌剤を開発できる可能性がある．

Wnt/β-カテニン系を特異的に阻害する医薬品はまだない．しかし，非ステロイド性抗炎症薬はシクロオキシゲナーゼ阻害のほか，Wnt/β-カテニン系を阻害することが報告されている．アスピリンやセレコキシブによる大腸癌抑制の一部に，この機序が関与している可能性がある．また，イマチニブはBcr-Ablチロシンキナーゼを標的とした慢性骨髄性白血病治療薬であるが，Wnt/β-カテニン系を阻害することも示されている．そのほか，レチノイン酸なども，この系を阻害する可能性がある．

著者らは，細胞性粘菌の分泌物質DIF(differentiation-inducing factor)の増殖抑制作用を調べているが，このおもな作用点はWnt/β-カテニン系で，しかもGSK-3βにきわめて近い．

DIFは種々の癌細胞で，GSK-3β活性化によりサイクリンD1とβ-カテニンをリン酸化し，これらの分解を促す[3,4]．β-カテニンの分解はサイクリンD1転写活性も低下させるため，DIFは蛋白質およびmRNAの両レベルでサイクリンD1を減少させる．

このようにDIFは，GSK-3β近傍に作用し，Wnt/β-カテニン系を強力に抑制する物質である．現在著者らは新規抗癌剤の開発を目標に，非臨床試験を行いつつある．

癌以外でGSK-3β活性化が治療につながる可能性があるのは心肥大である[5]．GSK-3βは心肥大を強力に抑制するが，圧負荷や成長因子などの刺激で，Ser^9リン酸化やWnt系活性化を介してGSK-3βは抑制され，心肥大が起こる．したがって，GSK-3β刺激薬を含むWnt/β-カテニン系抑制薬により，心肥大による心不全発症を予防できる可能性がある．

1) Meijer, L. et al.：Pharmacological inhibitors of glycogen syn-

thase kinase 3. *Trends Pharmacol. Sci.*, **25**：471-480, 2004.
2) Cohen, P. and Goedert, M.：GSK3 inhibitors：development and therapeutic potential. *Nat. Rev. Drug. Discov.*, **3**：479-487, 2004.
3) Takahashi-Yanaga, F. et al.：Dictyostelium differentiation-inducing factor-3 activates glycogen synthase kinase-3β and degrades cyclin D1 in mammalian cells. *J. Biol. Chem.*, **278**：9663-9670, 2003.
4) Takahashi-Yanaga, F. et al.：Involvement of GSK-3β and DYRK1B in differentiation-inducing factor-3-induced phosphorylation of cyclin D1 in HeLa cells. *J. Biol. Chem.*, **281**：38489-38497, 2006.
5) Blankesteijn, W. M. et al.：The Wnt/frizzled/GSK-3β pathway：a novel therapeutic target for cardiac hypertrophy. *Trends Pharmacol. Sci.*, **29**：175-180, 2008.

笹栗俊之／Toshiyuki SASAGURI
九州大学大学院医学研究院
生体情報科学講座臨床薬理学分野

糖尿病・内分泌代謝学

糖尿病合併症の原因となる異常骨髄細胞

Diabetic complication and bone marrow-derived cells

糖尿病人口は増加の一途をたどっており，現在日本においては糖尿病患者が820万人，糖尿病予備群が1,050万人で，40歳以上の3人に1人が予備群といわれている．糖尿病の合併症は，腎症，網膜症，神経障害の3大合併症以外に，脳血管障害，心筋梗塞，肝障害，皮膚疾患，閉塞性動脈硬化症など，広範な臓器障害をきたす．

著者らは最近の研究で糖尿病で起こる臓器障害が，骨髄由来の細胞と臓器細胞との異常な細胞融合現象が原因になることを明らかにした．高血糖が引き金になって，骨髄にプロインスリンとTNF-αを同時に産生する異常細胞が出現する．キメラマウスを用いた実験で，これらの異常骨髄細胞が末梢神経細胞や肝細胞と融合し，相手の細胞の遺伝子変異を起こして細胞傷害性に働くことを見出した[1-4]．

高血糖で多臓器に出現するプロインスリン陽性細胞

インスリン欠損型糖尿病モデル〔ストレプトゾトシン(STZ)投与マウス〕，高脂肪食負荷マウス，*ob/ob* マウスなどの種々の糖尿病モデル動物で，動物を糖尿病にするだけで，骨髄，末梢神経細胞，肝，脂肪組織，脾，胸腺など多くの臓器にプロインスリン陽性細胞が出現した[1]．これらプロインスリン細胞は血糖を下げる作用はなく，組織傷害性に働くサイトカインであるTNF-αを同時に産生することがわかった．すべての糖尿病モデル動物に共通の因子である高血糖状態がこの異常を引き起こす原因であるかどうかを調べるため，1日4回2時間ごとに腹腔内投与でブドウ糖負荷を行い，300 mg/dl以上の高血糖状態を断続的に起こすマウスモデルを作成した．このマウスで，ブドウ糖負荷開始後3日で骨髄，肝，脂肪組織，脾，胸腺にプロインスリン/TNF-α産生細胞が出現した．多臓器に出現するプロインスリン産生細胞は，造血細胞マーカーであるCD45を発現したため，骨髄由来である可能性が示唆された．そこでGFPマウスから骨髄移植を行い，レシピエントマウスを糖尿病にすると，多臓器に出現するプロインスリン/TNF-α陽性細胞は同時にGFPを発現しており，骨髄由来であることが判明した[1,4]．

糖尿病性末梢神経障害の原因となる骨髄細胞と後根神経節細胞との融合現象

糖尿病動物で，骨髄由来の細胞が標的臓器の細胞にどのような影響を与えるのかを調べるために，細胞自身が増殖や分裂を起こさない神経組織を第1に選択した．代表的な糖尿病合併症である末梢神経障害は脊髄後根神経節細胞のアポトーシスがおもな病態であるが，その原因の詳細は不明であった．

STZ糖尿病マウスで後根神経節にプロインスリン/TNF-α陽性細胞が出現し，ニューロンのマーカーのneurofilamentやSchwann細胞のマーカーのS100蛋白との二重染色により，プロインスリン/TNF-αは神経細胞とSchwann細胞に発現することがわかった．GFPマウスをドナーに，ROSAマウス(β-ガラクトシダーゼ過剰発現マウス)をレシピエントにして骨髄移植を行い，キメラマウスを作成したところ，糖尿病で出現するプロインスリン/TNF-α細胞はGFPとβ-ガラクトシダーゼを同時発現し，骨髄由来の細胞とレシピエントの神経細胞の細胞融合が示唆された．DNA ploidyの解析で，正常動物の後根神経節ニューロンはすべて2nであるのに対して，糖尿病動物の後根神経節ニューロンでは2nの細胞は87%で，4n，6n，8nの細胞が残りの13%を占め，プロインスリン/TNF-α陽性細胞の93%が4n以上の細胞であった．このことは脊髄後根神経節のプロインスリン/TNF-α産生細胞は，ほとんどすべて細胞融合したものと考えられる．融合細胞は細胞内カルシウムの代謝異常をきたし，高率でアポトーシスに陥ることがわかった．以上の結果より，糖尿病で起こる骨髄細胞と神経細胞との細胞融合は細胞の不可逆性の機能異常を引き起こし，進行性の末梢神経障害

平成 21 年度の研究成果の刊行に関する一覧

1. Matsuda T, Takahashi-Yanaga F, Yoshihara T, Maenaka K, Watanabe Y, Miwa Y, Morimoto S, Kubohara Y, Hirata M, Sasaguri T (2010) *Dictyostelium* differentiation-inducing factor-1 binds to mitochondrial malate dehydrogenase and inhibits its activity. J Pharmacol Sci. (in press)

2. Ohmine T, Miwa Y, Takahashi-Yanaga F, Morimoto S, Maehara Y, & Sasaguri T (2009) The involvement of aldosterone in cyclic stretch-mediated activation of NADPH oxidase in vascular smooth muscle cells. Hypertens Res. 32(8), 690-699

3. Zhan D-Y, Morimoto S, Du C-K, Wang Y-Y, Lu Q-W, Tanaka A, Ide T, Miwa Y, Takahashi-Yanaga F, & Sasaguri T (2009) Therapeutic effect of β-adrenoceptor blockers using a mouse model of dilated cardiomyopathy with a troponin mutation. Cardiovasc Res. 84(1), 64-71

4. Tadano N, Morimoto S, Takahashi- Yanaga F, Miwa Y, Ohtsuki I, & Sasaguri T (2009) Propyl gallate, a strong antioxidant, increases the Ca^{2+} sensitivity of cardiac myofilament. J Pharmacol Sci. 109(3), 456-458

5. Tanaka R, Miwa Y, Mou K, Tomikawa M, Eguchi N, Urade Y, Takahashi-Yanaga F, Morimoto S, Wake N, & Sasaguri T (2009) Knockout of the *l-pgds* gene aggravates obesity and atherosclerosis in mice. Biochem Biophys Res Commun. 378(4), 851-856

6. 笹栗俊之 (2009) GSK-3βと創薬. 医学のあゆみ 229(4), 293-294

7. Takahashi-Yanaga F & Sasaguri T (2009) Drug development targeting the glycogen synthase kinase-3β (GSK-3β)-mediated signal transduction pathway: Inhibitors of the Wnt/β-catenin signaling pathway as novel anticancer drugs. J Pharmacol Sci. 109(2), 179-183

Cardiovascular Research (2009) 84, 64–71
doi:10.1093/cvr/cvp168

EUROPEAN SOCIETY OF CARDIOLOGY®

Therapeutic effect of β-adrenoceptor blockers using a mouse model of dilated cardiomyopathy with a troponin mutation

Dong-Yun Zhan[1], Sachio Morimoto[1]*, Cheng-Kun Du[1], Yuan-Yuan Wang[1], Qun-Wei Lu[2], Atsushi Tanaka[3], Tomomi Ide[3], Yoshikazu Miwa[1], Fumi Takahashi-Yanaga[1], and Toshiyuki Sasaguri[1]

[1]*Department of Clinical Pharmacology, Faculty of Medical Sciences, Kyushu University, Fukuoka 812-8582, Japan;* [2]*Department of Physiology and Biophysics, Center for Cardiovascular Research, University of Illinois at Chicago, College of Medicine, Chicago, IL 60612, USA; and* [3]*Department of Cardiovascular Medicine, Faculty of Medical Sciences, Kyushu University, Fukuoka 812-8582, Japan*

Received 18 December 2008; revised 15 May 2009; accepted 21 May 2009; online publish-ahead-of-print 28 May 2009

Time for primary review: 31 days

KEYWORDS
Dilated cardiomyopathy;
β-Blocker;
Ventricular fibrillation;
Sudden death;
Survival

Aims Extensive clinical studies have demonstrated that β-adrenoceptor blocking agents (β-blockers) are beneficial in the treatment of chronic heart failure, which is due to various aetiologies, including idiopathic dilated cardiomyopathy (DCM) and ischaemic heart disease. However, little is known about the therapeutic efficacy of β-blockers in the treatment of the inherited form of DCM, of which causative mutations have recently been identified in various genes, including those encoding cardiac sarcomeric proteins. Using a mouse model of inherited DCM with a troponin mutation, we aim to study the treatment benefits of β-blockers.

Methods and results Three different types of β-blockers, carvedilol, metoprolol, and atenolol, were orally administered to a knock-in mouse model of inherited DCM with a deletion mutation ΔK210 in the cardiac troponin T gene (*TNNT2*). Therapeutic effects were examined on the basis of survival and myocardial remodelling. The lipophilic β_1-selective β-blocker metoprolol was found to prevent cardiac dysfunction and remodelling and extend the survival of knock-in mice. Conversely, both the non-selective β-blocker carvedilol and the hydrophilic β_1-selective β-blocker atenolol had no beneficial effects on survival and myocardial remodelling in this mouse model of inherited DCM.

Conclusion The highly lipophilic β_1-selective β-blocker metoprolol, known to prevent ventricular fibrillation via central nervous system-mediated vagal activation, may be especially beneficial to DCM patients showing a family history of frequent sudden cardiac death, such as those with a deletion mutation ΔK210 in the *TNNT2* gene.

1. Introduction

Dilated cardiomyopathy (DCM) is a cardiac muscle disorder characterized by ventricular chamber dilation and systolic dysfunction, which often leads to sudden death and heart failure.[1–3] Although DCM had been known to result from non-genetic insults, such as viruses, alcohol, toxins, and immunological injury, recent studies have revealed that mutations in genes for sarcolemmal transmembrane proteins, cytoskeletal proteins, nuclear envelope proteins, and sarcomeric proteins are also important causes of DCM.[4,5]

Patients affected by a deletion mutation ΔK210 in the cardiac troponin T gene (*TNNT2*), which has so far been identified in four unrelated families,[6–8] show a severe early-onset phenotype with a high incidence of sudden death and/or heart failure death. Recently, we created a knock-in mouse model of DCM using this mutation.[9] The knock-in mice developed markedly enlarged hearts with left ventricular (LV) systolic dysfunction and frequent sudden cardiac death, closely recapitulating the clinical phenotypes of human patients.

Several uncontrolled clinical studies provided the first evidence that metoprolol, a β_1-selective β-adrenoceptor blocking agent (β-blocker), had a beneficial clinical and haemodynamic effect in patients with heart failure due to idiopathic DCM.[10–13] Subsequent controlled clinical studies showed that metoprolol[14–20] and carvedilol, a non-selective β-blocker,[21–23] were both consistently beneficial to patients with symptomatic chronic heart failure due to idiopathic DCM or ischaemic heart disease. Comparisons between the effects of metoprolol and carvedilol therapy on cardiac performance reported that these two agents had parallel

* Corresponding author. Tel: +81 92 642 6081; fax: +81 92 642 6084.
E-mail address: morimoto@med.kyushu-u.ac.jp

beneficial effects in patients with chronic heart failure mostly due to ischaemic heart disease or idiopathic DCM.[24] Carvedilol was also later reported to have more beneficial effects in patients exclusively with idiopathic DCM.[25] The COMET study showed that carvedilol had a greater beneficial effect on survival than metoprolol when used to treat chronic heart failure mostly due to ischaemic heart disease or idiopathic DCM.[26]

In the present study, we sought to explore the therapeutic effects of metoprolol and carvedilol, as well as a low-lipophilic β-blocker, atenolol, on inherited DCM caused by a deletion mutation ΔK210 in the *TNNT2* gene, using a knock-in mouse model. We found that the highly lipophilic β_1-selective β-blocker metoprolol, but not the lipophilic non-selective β-blocker carvedilol or the hydrophilic β_1-selective β-blocker atenolol, was able to extend survival in DCM mice and prevent cardiac remodelling and dysfunction. This may be due to the blockade of central nervous β_1-adrenoceptors modulating vagal nervous outflow.

2. Methods

2.1 Animal model

A knock-in mouse model, in which three base-pairs coding for K210 in cTnT were deleted from the endogenous gene *TNNT2*, was created as described previously.[9] Homozygous mutant mice were used for the DCM model. The investigation conforms with the *Guide for the Care and Use of Laboratory Animals* published by the US National Institutes of Health (NIH Publication No. 85-23, revised 1996). The experimental protocol was reviewed by the Committee of Ethics on Animal Experiments at the Faculty of Medicine, Kyushu University, and carried out according to the *Guidelines for Animal Experiments*, Faculty of Medicine, Kyushu University, and The Law (No. 105) and Notification (No. 6) of the Japanese Government.

2.2 Drug administration

Carvedilol was supplied by Nippon DAIICHI SANKYO Co., Ltd (Japan). (±)-Metoprolol (+)-tartrate salt was purchased from Sigma (USA). Atenolol was purchased from Wako Pure Chemical Industries, Ltd (Japan). From 30 days of age, metoprolol, carvedilol, or atenolol, suspended in 0.25% methylcellulose solution, was administered orally once daily to DCM mice; control mice received vehicles only. The doses for each of the drugs were selected on the basis of a comparable suppression of heart rate.

2.3 Electrocardiography, echocardiography, and blood pressure measurements

Surface electrocardiography (ECG) (standard limb lead II) and transthoracic echocardiography (M-mode) were measured after sodium pentobarbital administration (50 mg/kg, i.p.) using, respectively, an ECG processor SP-2000 (Softron, Japan) and a 14 MHz linear array probe with a diagnostic ultrasound system, Nemio SSA-550A (Toshiba, Japan). Blood pressure was measured in conscious mice using a computerized non-invasive tail-cuff system BP-98A (Softron, Japan).

2.4 Histochemistry

The hearts, excised from mice anaesthetized with pentobarbital (50 mg/kg, i.p.), were fixed in a 10% formalin neutral buffered solution after perfusion with oxygenated Krebs–Henseleit solution (118 mM NaCl, 4.7 mM KCl, 1.2 mM MgSO4, 1.2 mM KH2PO4, 25 mM NaHCO3, 2.5 mM CaCl2, 0.5 mM EDTA-Na2, 10 mM HEPES, 11 mM D-glucose) containing 50 mM 2,3-butanedione monoxime in a Langendorff mode at 37°C. Fixed hearts were cut transversely at the mid-ventricular level, embedded in paraffin, sectioned at 5 μm, and stained with azan. The extent of fibrosis in LV myocardium was quantified using the ImageJ program from NIH for three cardiac sections from each mouse.

2.5 Respiratory sinus arrhythmia

The trachea was cannulated under light anaesthesia with ether, and the mice were mechanically ventilated with 100% room air (tidal volume 0.5 mL, 120 inflations/min). At 10 min after the administration of D-tubocurarine (3 mg/kg, i.p.), surface ECG (standard limb lead II) was recorded three times for 20 s every 5 min under unanaesthetized conditions. The standard deviation of the R-R intervals per respiratory cycle (SD R-R), as an index of vagal activity,[27,28] was calculated on the basis of the mean of 120 respiratory cycles in each mouse.

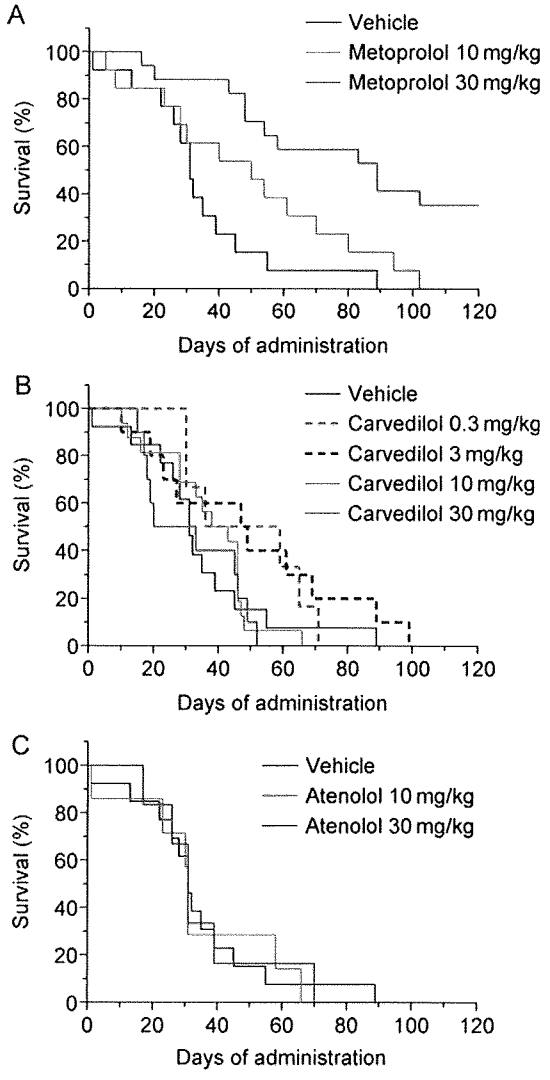

Figure 1 Effects of β-blockers on the survival of a mouse model of inherited DCM caused by a deletion mutation ΔK210 in the *TNNT2* gene. From 30 days of age, metoprolol (10 mg/kg, $n = 13$; 30 mg/kg, $n = 17$) (*A*), carvedilol (0.3 mg/kg, $n = 6$; 3 mg/kg, $n = 10$; 10 mg/kg, $n = 16$; 30 mg/kg, $n = 10$) (*B*) and atenolol (10 mg/kg, $n = 7$; 30 mg/kg, $n = 6$) (*C*), and vehicle only (methylcellulose, $n = 13$) were administered to DCM mice orally once daily. Kaplan–Meier survival curves indicate that mice treated with metoprolol at 30 mg/kg per day have significantly longer life spans than mice treated with vehicle only (log-rank test, $P = 0.0002$).

2.6 Western blot analysis

After a brief perfusion of the isolated heart with oxygenated Krebs-Henseleit solution at 37°C in a Langendorff mode to remove blood from the myocardium, ventricles were dissected from the heart, blotted on filter paper, and homogenized in Laemmli's sample buffer. LV homogenate samples were subjected to western blot analysis as described previously.[29] Expression levels of brain natriuretic peptide (BNP) were determined using an anti-proBNP polyclonal antibody (ab32842; Abcam) and an anti-GAPDH monoclonal antibody (ab9484; Abcam). Signals were visualized using SuperSignal West Femto Maximum Sensitivity Substrate (Thermo Scientific) and Hyperfilm ECL (GE Healthcare) and were quantified using GAPDH signal as a protein loading control. Similarly, relative phosphorylation levels of phospholamban (PLB) were obtained by normalizing the signals of the PLB band, probed with anti-phospho-PLB-Ser16 polyclonal antibody (ab15000; Abcam), to that probed with anti-PLB monoclonal antibody (ab2865; Abcam).

2.7 Myosin isoform contents

Myosin heavy chain (MyHC) isoforms in the LV myocardium were separated on SDS-PAGE according to the method outlined in Rundell *et al.*,[30] and relative β-isoform expression (percentage of total MyHC) was determined by an optical densitometric scan using Phoretix gel analysis software (Phoretix International, UK).

3. Results

DCM mice with a deletion mutation ΔK210 in the *TNNT2* gene show a very high mortality due to sudden cardiac death without showing overt heart failure symptoms, such as decreased spontaneous movement activity and dyspnoea, up to, at least, a day before their death.[9] Oral administration of the β_1-selective β-blocker metoprolol (10–30 mg/kg per day) was found to extend the survival of

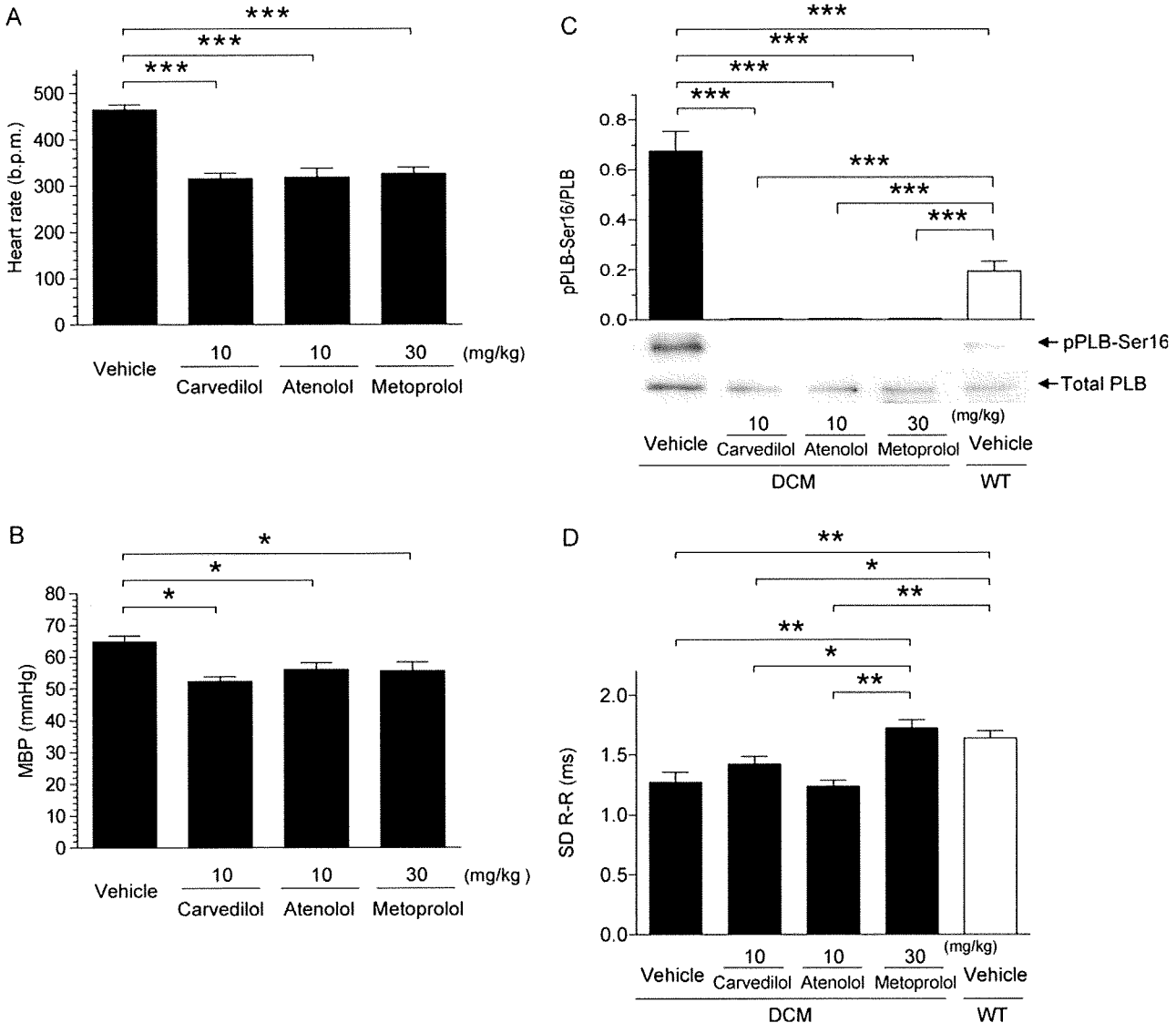

Figure 2 Effects of β-blockers on cardiac autonomic nervous activity in DCM mice with a deletion mutation ΔK210 in the *TNNT2* gene. (*A*) Chronotropic effects of β-blockers on DCM mice. Heart rates were determined by echocardiography under anaesthesia (30 mg/kg of pentobarbital, i.p.). Data represent the means ± SE for five mice. (*B*) Hypotensive effects of β-blockers on DCM mice. Mean blood pressures (MBP) were determined under conscious conditions. Data represent the means ± SE for four mice. (*C*) Effects of β-blockers on the phosphorylation level of phospholamban (PLB) in the LV myocardium of DCM mice. The phosphorylation level of PLB was determined by western blot analysis of the hearts. Data represent the means ± SE for three mice. (*D*) Effects of β-blockers on the standard deviation of the mean of the R-R intervals (SD R-R). Data represent the means ± SE for three mice. All data were obtained at 2 h after a single oral administration of β-blocker or vehicle only to 2-month-old untreated mice. Statistical significance was determined by ANOVA followed by *post hoc* Newman-Keuls multiple comparison test. $^*P < 0.05$, $^{**}P < 0.01$, $^{***}P < 0.001$. Note that pairs with no significant differences are not indicated.

DCM mice in a dose-dependent manner (*Figure 1A*). In contrast, oral administration of the non-selective β-blocker carvedilol had no significant effects on the survival of DCM mice at a dose showing a similar time-course of pharmacodynamic effect on heart rate as the effective dose of metoprolol (*Figure 1B*) (see also Supplementary materials online, *Figure S1*). Although lower doses of carvedilol showed some trend to slightly extend the survival of DCM mice, no statistically significant differences were demonstrated against the control vehicle. These results suggest that β_1-selectivity may be beneficial in extending survival. However, another β_1-selective β-blocker, atenolol, also had no significant effect on the survival of DCM mice at a dose showing a similar time-course of pharmacodynamic effect on heart rate as the effective dose of metoprolol (*Figure 1C*). Carvedilol and atenolol had significant negative chronotropic and hypotensive effects on DCM mice even at non-beneficial doses, which were comparable to those exerted by a beneficial dose of metoprolol (*Figure 2A* and *B*). Phosphorylation of Ser16 of PLB in the heart was significantly increased in DCM mice, and it was completely inhibited by any of the three β-blockers (*Figure 2C*). These results indicate that the three β-blockers exert equivalent levels of sympathetic blockade, independent of their effects on the survival of DCM mice. The respiratory sinus arrhythmia in artificially ventilated DCM mice was measured by determining the variability of R-R interval of the ECG per respiratory cycle (SD R-R), which has been shown to reflect the tonic activation of the efferent cardiac vagal nerves (*Figure 2D*).[27,28] DCM mice had significantly smaller SD R-R than wild-type mice. Metoprolol, but not carvedilol or atenolol, was found to significantly increase the SD R-R in DCM mice, consistent with the findings that metoprolol could activate the vagal nervous outflow to the heart, possibly due to the inhibition of β_1-adrenoceptor in the central nervous system.[31]

DCM mice commonly have electrophysiological abnormality in the heart with long QT, which might be involved in their frequent sudden death.[9] Metoprolol was found to shorten the QT interval significantly at 30 mg/kg per day, whereas carvedilol and atenolol had no significant effects on the QT interval of DCM mice (*Table 1*). DCM mice also commonly showed decreased amplitude of S-wave and a widened QRS complex in the ECG results. Metoprolol, but not carvedilol or atenolol, reduced these ECG abnormalities (*Table 1*).

DCM mice developed markedly enlarged hearts with ventricular dilation and significant interstitial fibrosis in the myocardium (*Figure 3*). Oral administration of metoprolol prevented the cardiac remodelling and fibrosis in a dose-dependent manner (*Figure 3*), with the heart-to-body weight ratio (*Table 2*) and fibrosis area (*Figure 3B*) showing a significant decrease at 30 mg/kg per day. Carvedilol and atenolol had no anti-remodelling and anti-fibrotic effects on the hearts of DCM mice.

DCM mice had LV systolic dysfunction and dilation, as were evident from reduced LV ejection fraction (EF) and increased LV end-diastolic dimension (LVEDD), respectively (*Table 3*). Metoprolol improved LV systolic function of DCM mice in a dose-dependent manner while reducing LV dilation (*Table 3*); metoprolol increased EF significantly at 30 mg/kg per day while significantly reducing LVEDD. Carvedilol and atenolol had no beneficial effects on LV systolic function and structure in DCM mice. DCM mice had significantly lower blood pressures than wild-type mice, and only metoprolol restored the blood pressure to normal levels (*Table 3*). Metoprolol, but not carvedilol or atenolol, decreased the myocardial expression of BNP and β-myosin heavy chain—biomarkers of heart failure—in a dose-dependent manner (*Figure 4*), indicating that metoprolol has a beneficial effect on cardiac function in DCM mice.

Table 1 ECG (standard limb lead II) data in DCM or WT mice with vehicle or β-blocker treatment

	DCM						WT (vehicle)
	Vehicle	Carvedilol		Atenolol (10 mg/kg)	Metoprolol		
		10 mg/kg	30 mg/kg		10 mg/kg	30 mg/kg	
Age, weeks	8	8	8	8	8	8	8
Number of mice	5	5	5	4	5	5	5
HR, b.p.m.	338 ± 6	337 ± 8	321 ± 8	341 ± 22	349 ± 6	334 ± 7	341 ± 10
P, mV/100	0.17 ± 0.02	0.18 ± 0.02	0.16 ± 0.02	0.14 ± 0.05	0.16 ± 0.02	0.18 ± 0.02	0.17 ± 0.02
R, mV/100	1.64 ± 0.12	1.60 ± 0.12	1.35 ± 0.16	1.63 ± 0.17	1.46 ± 0.09	1.43 ± 0.17	1.53 ± 0.09
S, mV/100	−0.04 ± 0.01***	−0.04 ± 0.01***	−0.04 ± 0.02***	−0.11 ± 0.01***	−0.17 ± 0.02***	−0.22 ± 0.01***,†	−0.51 ± 0.09
T, mV/100	0.03 ± 0.01***	0.02 ± 0.01***	0.02 ± 0.01***	0.03 ± 0.02***	0.05 ± 0.01***	0.07 ± 0.01***,†	0.17 ± 0.01
QRS, ms	19.6 ± 0.5***	19.2 ± 0.7***	20.6 ± 0.5***	20.6 ± 0.8***	18.2 ± 0.9***	15.0 ± 0.7**,†††	12.2 ± 0.6
PR, ms	46 ± 2	46 ± 2	47 ± 2	45 ± 2	44 ± 1	41 ± 3	43 ± 2
QT, ms	59 ± 4**	55 ± 4*	57 ± 5**	61 ± 4**	52 ± 4*	39 ± 3†	36 ± 4

Vehicle only (methylcellulose) or β-blockers were administered to mice orally for 28 days from 30 days of age. Surface ECG was measured at ~24 h after the last administration. Data represent the means ± SE. Statistical significance was determined by ANOVA followed by *post hoc* Newman–Keuls multiple comparison test.

WT, wild-type; DCM, DCM mice; HR, heart rate; b.p.m., beats per minute.

*$P < 0.05$, **$P < 0.01$, ***$P < 0.001$ vs. vehicle-treated WT mice.

†$P < 0.05$, †††$P < 0.001$ vs. vehicle-treated DCM mice.

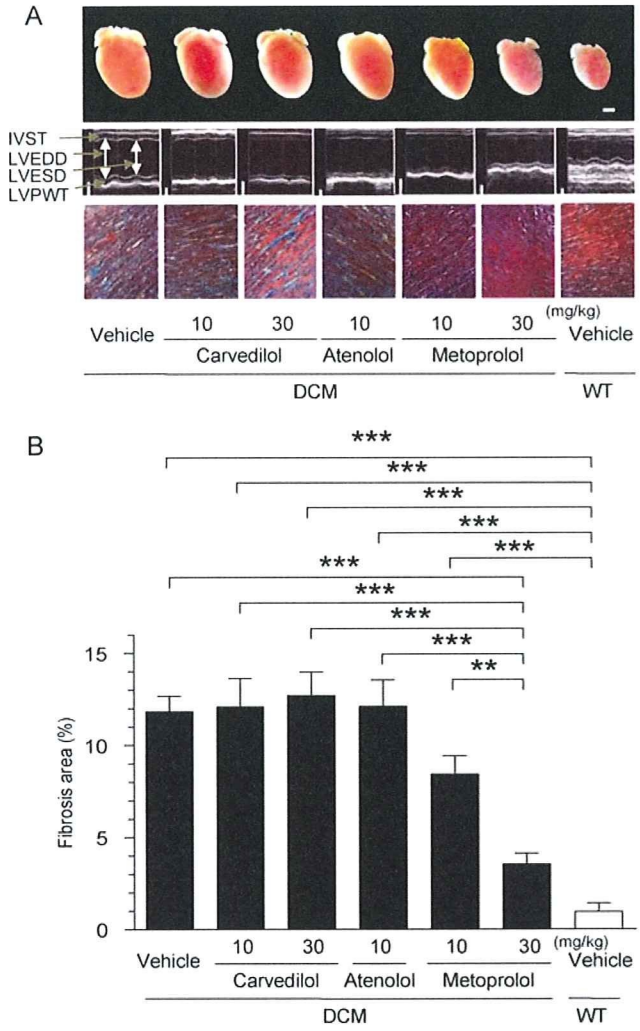

Figure 3 Effects of β-blockers on cardiac remodelling and function in DCM mice with a deletion mutation ΔK210 in the *TNNT2* gene. From 30 days of age, β-blocker or vehicle only was administered to mice orally once daily for 28 days. (*A*) Transthoracic echocardiography images (middle images) were measured at ~24 h after the last administration, and the hearts were then excised to analyse their gross morphology (top images; scale bar 2 mm) and the histology of the LV myocardium (bottom images; connective tissues were stained blue with azan). (*B*) Quantitative analysis of the fibrosis area in the LV myocardium. Data represent the means ± SE for three mice. Statistical significance was determined by ANOVA followed by *post hoc* Newman–Keuls multiple comparison test. $^{**}P < 0.01$, $^{***}P < 0.001$. Note that pairs with no significant differences are not indicated.

4. Discussion

Metoprolol, a second-generation β-blocker with β_1-selective blockade action, has been demonstrated to improve haemodynamic status and symptoms and reduce cardiac transplantation and all causes of mortality in patients with idiopathic DCM.[10–13,17–20,32] In the present study, we found that metoprolol improved cardiac systolic function, prevented cardiac remodelling and sudden death, and extended the survival of a mouse model of DCM with a deletion mutation ΔK210 in the *TNNT2* gene. These findings strongly suggest that a common pathogenic mechanism targeted by metoprolol may exist between this genetic model of DCM and idiopathic DCM. Carvedilol, a third-generation β-blocker with non-selective β-blockade, α1-blockade, and antioxidant actions, has also been shown to improve LV systolic function,

Table 2 Heart weight data in DCM or WT mice with vehicle or β-blocker treatment

	DCM								WT (vehicle)
	Vehicle	Carvedilol		Atenolol		Metoprolol			
		10 mg/kg	30 mg/kg	10 mg/kg	30 mg/kg	10 mg/kg	30 mg/kg		
Age, weeks	8	8	8	8	8	8	8		8
Number of mice	5	6	7	4	4	7	5		5
BW, g	21.2 ± 0.7	20.7 ± 1.1	20.4 ± 0.5	21.6 ± 1.0	19.8 ± 0.3	21.9 ± 0.5	21.8 ± 1.3		20.3 ± 0.6
HW, mg	243.2 ± 14.9***	246.2 ± 11.1***	250.5 ± 11.1***	240.1 ± 19.0***	228.3 ± 16.9***	206.8 ± 10.7***	176.7 ± 12.2***,††		111.1 ± 3.3
HW/BW, mg/g	11.5 ± 0.6***	12.3 ± 1.1***	12.3 ± 0.3***	11.3 ± 1.3***	11.5 ± 0.8***	9.5 ± 0.6***	8.1 ± 0.4*,†		5.5 ± 0.1

Vehicle only (methylcellulose) or β-blockers were administered to mice orally for 28 days from 30 days of age. Body weight and heart weight were determined at ~24 h after the last administration. Data represent the means ± SE. Statistical significance was determined by ANOVA followed by *post hoc* Newman–Keuls Multiple Comparison Test.
BW, body weight; HW, heart weight; HW/BW, heart weight-to-body weight ratio.
$^{*}P < 0.05$, $^{***}P < 0.001$ vs. vehicle-treated WT mice.
$^{\dagger}P < 0.05$, $^{\dagger\dagger}P < 0.01$ vs. vehicle-treated DCM mice.

Table 3 Echocardiography and blood pressure data in DCM or WT mice with vehicle or β-blocker treatment

	DCM						WT (vehicle)
	Vehicle	Carvedilol		Atenolol (10 mg/kg)	Metoprolol		
		10 mg/kg	30 mg/kg		10 mg/kg	30 mg/kg	
Age, weeks	8	8	8	8	8	8	8
Echocardiography							
Number of mice	5	6	6	4	6	8	7
HR, b.p.m.	383 ± 4	377 ± 8	370 ± 7	396 ± 9	393 ± 4	379 ± 8	393 ± 4
IVST, mm	0.45 ± 0.02	0.41 ± 0.01	0.40 ± 0.02	0.45 ± 0.03	0.42 ± 0.02	0.40 ± 0.03	0.48 ± 0.03
LVESD, mm	4.95 ± 0.18***	5.00 ± 0.20***	5.39 ± 0.25***	4.63 ± 0.16***	4.25 ± 0.23***	3.88 ± 0.16***,††	2.32 ± 0.22
LVEDD, mm	5.80 ± 0.19***	5.57 ± 0.18***	6.11 ± 0.20***	5.45 ± 0.12***	5.17 ± 0.14***	4.87 ± 0.15***,††	3.62 ± 0.23
LVPWT, mm	0.46 ± 0.02	0.41 ± 0.01	0.40 ± 0.02	0.43 ± 0.03	0.42 ± 0.02	0.42 ± 0.01	0.45 ± 0.02
FS, %	14.8 ± 1.6***	12.0 ± 1.0***	11.7 ± 1.4***	14.8 ± 2.1***	17.8 ± 2.3***	21.8 ± 1.1***,†	37.9 ± 2.2
EF, %	38.6 ± 2.7***	30.0 ± 2.3***	28.8 ± 3.1***	36.8 ± 4.1***	42.3 ± 4.7***	49.4 ± 2.1***,†	74.3 ± 2.6
Blood pressure							
Number of mice	4	4	ND	4	ND	4	4
MBP	64.75 ± 2.02**	63.75 ± 1.80**	ND	66.00 ± 1.41*	ND	71.50 ± 1.04†	73.75 ± 2.06

Vehicle only (methylcellulose) or β-blockers were administered to mice orally for 28 days from 30 days of age, and transthoracic echocardiography and blood pressure were measured at ~24 h after the last administration. Data represent the means ± SE. Statistical significance was determined by ANOVA followed by *post hoc* Newman–Keuls multiple comparison test.

IVST, interventricular septal wall thickness; LVPWT, LV posterior wall thickness; LV, left ventricular; LVESD, LV end-systolic dimension; LVEDD, LV end-diastolic dimension; FS, fractional shortening; EF, ejection fraction; MBP, mean blood pressure. ND, not determined.

*$P < 0.05$, **$P < 0.01$, ***$P < 0.001$ vs. vehicle-treated WT mice.

†$P < 0.05$, ††$P < 0.01$ vs. vehicle-treated DCM mice.

heart failure symptoms, endothelium-dependent vasodilation, and coronary microvascular function in patients with exclusively idiopathic DCM.[22,23,33–35] Furthermore, carvedilol has been shown to have a higher beneficial effect on survival than metoprolol in patients with chronic heart failure, which is mostly due to ischaemic heart disease or idiopathic DCM (reported in the COMET study[26]). In the present study, however, carvedilol had no beneficial effects on cardiac systolic function, cardiac remodelling, sudden death, and survival in the mouse model of DCM. Although it is very difficult to directly compare the results from clinical study and animal model study, this somewhat surprising result might be related to the differences in the study design. In the clinical studies, carvedilol is added to the standard therapy with diuretics, angiotensin-converting enzyme inhibitors, and/or digoxin, with its dose being gradually increased to the target dose, although this was not the case in our animal model study. Carvedilol, in fact, may not have had such a beneficial effect on non-ischaemic cardiomyopathy, as an analysis of the COMET study shows that vascular protection by carvedilol contributes to its superior effects in the treatment of heart failure compared with metoprolol.[36] Of note is that carvedilol, but not metoprolol, blocks HERG potassium channels and should have a QT prolonging effect.[37,38] This might be responsible for the lack of beneficial effect of carvedilol on our mouse model, since this model already has a significantly prolonged QT interval. Future studies are required to explore these possibilities.

The present study also showed that in contrast to metoprolol, another β_1-selective β-blocker, atenolol, had no beneficial effects on cardiac systolic function, cardiac remodelling, and survival in the mouse model of DCM. Metoprolol and atenolol have equivalent potency and selectivity for β_1-blockade with similar pharmacokinetics. However, atenolol is not recommended for the treatment of heart failure and is currently approved as an antihypertensive and anti-ischaemic drug. Atenolol is hydrophilic, however, β-blockers, which have a beneficial effect in heart failure treatment, have in common some degree of lipophilicity.[39] Highly lipophilic β-blockers, including metoprolol, can easily cross the blood–brain barrier,[40] so they could block the β-adrenoceptors in the brain and decrease sympathetic outflow to the heart, which has been shown to play an important role in the progression of heart failure.[41,42] In the present study, however, carvedilol, which has a moderate lipophilicity,[39] was not able to prevent cardiac remodelling and dysfunction and extend survival in the mouse model of DCM. The three β-blockers tested in this study can cause equivalent levels of sympathetic blockade in DCM mice, making it, furthermore, unlikely that the decreased sympathetic outflow to the heart could be a relevant mechanism for the beneficial effect of metoprolol. Of note is that this mouse model of DCM shows almost no overt congestive heart failure symptoms but develops a frequent sudden death due to ventricular fibrillation (VF).[9] Interestingly, a recent animal model study has shown that metoprolol can reduce the incidence of VF after coronary artery occlusion by a better maintained vagal activation, compared with atenolol. This suggests that the blockade of central nervous β_1-adrenoceptors modulating vagal nervous outflow is of importance for the prevention of VF and sudden cardiac death.[31] In the present study, metoprolol, but not atenolol or carvedilol, was found to induce a tonic activation of the efferent cardiac vagal nerves in DCM mice, probably due to β_1-blockade in the central nervous system, and prevent sudden cardiac death. Mechanisms by which long-term metoprolol treatment improves the cardiac systolic function and prevents cardiac remodelling in DCM mice remain unclear. However, since it is unlikely that metoprolol can directly increase myocardial contractility, a reduction in preload due to the decreased end-diastolic LV volume may,

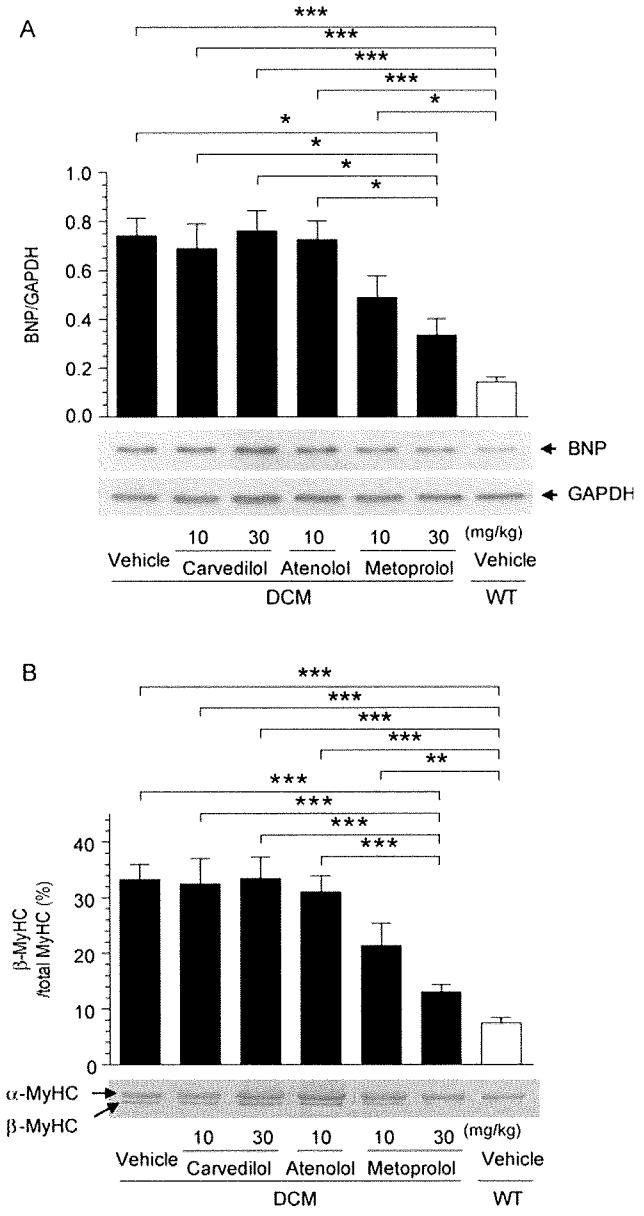

Figure 4 Effects of β-blockers on the expression levels of heart failure markers in the LV myocardium of DCM mice with a deletion mutation ΔK210 in the *TNNT2* gene. From 30 days of age, β-blocker or vehicle only was administered to mice orally once daily for 28 days. The hearts were excised at ~24 h after the last administration to determine the expression levels of pro-BNP (*A*) and β-MyHC (*B*). Data represent the means ± SE for four and five mice in panels A and B, respectively. Statistical significance was determined by ANOVA followed by *post hoc* Newman–Keuls multiple comparison test. $^{*}P < 0.05$, $^{**}P < 0.01$, $^{***}P < 0.001$. Note that pairs with no significant differences are not indicated.

at least in part, contribute to the moderately increased EF after long-term metoprolol treatment. Prevention of the cardiac remodelling could also contribute to the lack of progressive electrophysiological deterioration observed in treated mice. Finally, the present study suggests that the β_1-selective lipophilic β-blocker metoprolol, which could prevent VF via central nervous system-mediated vagal activation, might have an especially important benefit to inherited DCM patients showing frequent sudden death, such as those affected by a deletion mutation ΔK210 in the *TNNT2* gene.[6–8]

Supplementary material

Supplementary material is available at *Cardiovascular Research* online.

Conflict of interest: none declared.

Funding

This work was supported by Grants-in-Aid for Science Research (17300129) from the Japan Society for the Promotion of Science (JSPS) and grants from the Vehicle Racing Commemorative Foundation and the Mitsubishi Pharma Research Foundation to S.M. C.-K.D. is a recipient of the JSPS Postdoctoral Fellowship for Foreign Researchers.

References

1. Dec GW, Fuster V. Idiopathic dilated cardiomyopathy. *N Engl J Med* 1994; **331**:1564–1575.
2. Kasper EK, Agema WR, Hutchins GM, Deckers JW, Hare JM, Baughman KL. The causes of dilated cardiomyopathy: a clinicopathologic review of 673 consecutive patients. *J Am Coll Cardiol* 1994;**23**:586–590.
3. Manolio TA, Baughman KL, Rodeheffer R, Pearson TA, Bristow JD, Michels VV *et al.* Prevalence and etiology of idiopathic dilated cardiomyopathy (summary of a National Heart, Lung, and Blood Institute workshop). *Am J Cardiol* 1992;**69**:1458–1466.
4. Fatkin D, Graham RM. Molecular mechanisms of inherited cardiomyopathies. *Physiol Rev* 2002;**82**:945–980.
5. Morimoto S. Sarcomeric proteins and inherited cardiomyopathies. *Cardiovasc Res* 2008;**77**:659–666.
6. Mogensen J, Murphy RT, Shaw T, Bahl A, Redwood C, Watkins H *et al.* Severe disease expression of cardiac troponin C and T mutations in patients with idiopathic dilated cardiomyopathy. *J Am Coll Cardiol* 2004;**44**:2033–2040.
7. Kamisago M, Sharma SD, DePalma SR, Solomon S, Sharma P, McDonough B *et al.* Mutations in sarcomere protein genes as a cause of dilated cardiomyopathy. *N Engl J Med* 2000;**343**:1688–1696.
8. Hanson EL, Jakobs PM, Keegan H, Coates K, Bousman S, Dienel NH *et al.* Cardiac troponin T lysine 210 deletion in a family with dilated cardiomyopathy. *J Card Fail* 2002;**8**:28–32.
9. Du CK, Morimoto S, Nishii K, Minakami R, Ohta M, Tadano N *et al.* Knock-in mouse model of dilated cardiomyopathy caused by troponin mutation. *Circ Res* 2007;**101**:185–194.
10. Swedberg K, Hjalmarson A, Waagstein F, Wallentin I. Beneficial effects of long-term beta-blockade in congestive cardiomyopathy. *Br Heart J* 1980; **44**:117–133.
11. Swedberg K, Hjalmarson A, Waagstein F, Wallentin I. Adverse effects of beta-blockade withdrawal in patients with congestive cardiomyopathy. *Br Heart J* 1980;**44**:134–142.
12. Waagstein F, Caidahl K, Wallentin I, Bergh CH, Hjalmarson A. Long-term beta-blockade in dilated cardiomyopathy. Effects of short- and long-term metoprolol treatment followed by withdrawal and readministration of metoprolol. *Circulation* 1989;**80**:551–563.
13. Heilbrunn SM, Shah P, Bristow MR, Valantine HA, Ginsburg R, Fowler MB. Increased beta-receptor density and improved hemodynamic response to catecholamine stimulation during long-term metoprolol therapy in heart failure from dilated cardiomyopathy. *Circulation* 1989;**79**:483–490.
14. MERIT-HF Study Group. Effect of metoprolol CR/XL in chronic heart failure: Metoprolol CR/XL Randomised Intervention Trial in Congestive Heart Failure (MERIT-HF). *Lancet* 1999;**353**:2001–2007.
15. The RESOLVD Investigators. Effects of metoprolol CR in patients with ischemic and dilated cardiomyopathy: the randomized evaluation of strategies for left ventricular dysfunction pilot study. *Circulation* 2000; **101**:378–384.
16. Groenning BA, Nilsson JC, Sondergaard L, Fritz-Hansen T, Larsson HB, Hildebrandt PR. Antiremodeling effects on the left ventricle during beta-blockade with metoprolol in the treatment of chronic heart failure. *J Am Coll Cardiol* 2000;**36**:2072–2080.
17. Engelmeier RS, O'Connell JB, Walsh R, Rad N, Scanlon PJ, Gunnar RM. Improvement in symptoms and exercise tolerance by metoprolol in patients with dilated cardiomyopathy: a double-blind, randomized, placebo-controlled trial. *Circulation* 1985;**72**:536–546.

18. Waagstein F, Bristow MR, Swedberg K, Camerini F, Fowler MB, Silver MA *et al.* Beneficial effects of metoprolol in idiopathic dilated cardiomyopathy. Metoprolol in Dilated Cardiomyopathy (MDC) Trial Study Group. *Lancet* 1993;**342**:1441-1446.
19. Andersson B, Hamm C, Persson S, Wikstrom G, Sinagra G, Hjalmarson A *et al.* Improved exercise hemodynamic status in dilated cardiomyopathy after beta-adrenergic blockade treatment. *J Am Coll Cardiol* 1994;**23**: 1397-1404.
20. Andersson B, Caidahl K, di Lenarda A, Warren SE, Goss F, Waldenstrom A *et al.* Changes in early and late diastolic filling patterns induced by long-term adrenergic beta-blockade in patients with idiopathic dilated cardiomyopathy. *Circulation* 1996;**94**:673-682.
21. Packer M, Bristow MR, Cohn JN, Colucci WS, Fowler MB, Gilbert EM *et al.* The effect of carvedilol on morbidity and mortality in patients with chronic heart failure. U.S. Carvedilol Heart Failure Study Group. *N Engl J Med* 1996;**334**:1349-1355.
22. Metra M, Nardi M, Giubbini R, Dei Cas L. Effects of short- and long-term carvedilol administration on rest and exercise hemodynamic variables, exercise capacity and clinical conditions in patients with idiopathic dilated cardiomyopathy. *J Am Coll Cardiol* 1994;**24**:1678-1687.
23. Chizzola PR, Freitas HF, Caldas MA, da Costa JM, Meneghetti C, Marinho NV *et al.* Effects of carvedilol in heart failure due to dilated cardiomyopathy. Results of a double-blind randomized placebo-controlled study (CARIBE study). *Arq Bras Cardiol* 2000;**74**:233-242.
24. Kukin ML, Kalman J, Charney RH, Levy DK, Buchholz-Varley C, Ocampo ON *et al.* Prospective, randomized comparison of effect of long-term treatment with metoprolol or carvedilol on symptoms, exercise, ejection fraction, and oxidative stress in heart failure. *Circulation* 1999;**99**:2645-2651.
25. Metra M, Giubbini R, Nodari S, Boldi E, Modena MG, Dei Cas L. Differential effects of beta-blockers in patients with heart failure: A prospective, randomized, double-blind comparison of the long-term effects of metoprolol versus carvedilol. *Circulation* 2000;**102**:546-551.
26. Poole-Wilson PA, Swedberg K, Cleland JG, Di Lenarda A, Hanrath P, Komajda M *et al.* Comparison of carvedilol and metoprolol on clinical outcomes in patients with chronic heart failure in the Carvedilol Or Metoprolol European Trial (COMET): randomised controlled trial. *Lancet* 2003; **362**:7-13.
27. Potter EK. Inspiratory inhibition of vagal responses to baroreceptor and chemoreceptor stimuli in the dog. *J Physiol* 1981;**316**:177-190.
28. Rozanski A, Blumenthal JA, Kaplan J. Impact of psychological factors on the pathogenesis of cardiovascular disease and implications for therapy. *Circulation* 1999;**99**:2192-2217.
29. Nakaura H, Morimoto S, Yanaga F, Nakata M, Nishi H, Imaizumi T *et al.* Functional changes in troponin T by a splice donor site mutation that causes hypertrophic cardiomyopathy. *Am J Physiol* 1999;**277**:C225-C232.
30. Rundell VL, Geenen DL, Buttrick PM, de Tombe PP. Depressed cardiac tension cost in experimental diabetes is due to altered myosin heavy chain isoform expression. *Am J Physiol Heart Circ Physiol* 2004;**287**: H408-H413.
31. Ablad B, Bjuro T, Bjorkman JA, Edstrom T. Prevention of ventricular fibrillation requires central beta-adrenoceptor blockade in rabbits. *Scand Cardiovasc J* 2007;**41**:221-229.
32. Di Lenarda A, De Maria R, Gavazzi A, Gregori D, Parolini M, Sinagra G *et al.* Long-term survival effect of metoprolol in dilated cardiomyopathy. The SPIC (Italian Multicentre Cardiomyopathy Study) Group. *Heart* 1998;**79**:337-344.
33. Patrianakos AP, Parthenakis FI, Mavrakis HE, Diakakis GF, Chlouverakis GI, Vardas PE. Comparative efficacy of nebivolol versus carvedilol on left ventricular function and exercise capacity in patients with nonischemic dilated cardiomyopathy. A 12-month study. *Am Heart J* 2005;**150**:985.
34. Nishioka K, Nakagawa K, Umemura T, Jitsuiki D, Ueda K, Goto C *et al.* Carvedilol improves endothelium-dependent vasodilation in patients with dilated cardiomyopathy. *Heart* 2007;**93**:247-248.
35. Neglia D, De Maria R, Masi S, Gallopin M, Pisani P, Pardini S *et al.* Effects of long-term treatment with carvedilol on myocardial blood flow in idiopathic dilated cardiomyopathy. *Heart* 2007;**93**:808-813.
36. Remme WJ, Torp-Pedersen C, Cleland JG, Poole-Wilson PA, Metra M, Komajda M *et al.* Carvedilol protects better against vascular events than metoprolol in heart failure: results from COMET. *J Am Coll Cardiol* 2007;**49**:963-971.
37. Karle CA, Kreye VA, Thomas D, Rockl K, Kathofer S, Zhang W *et al.* Antiarrhythmic drug carvedilol inhibits HERG potassium channels. *Cardiovasc Res* 2001;**49**:361-370.
38. Kawakami K, Nagatomo T, Abe H, Kikuchi K, Takemasa H, Anson BD *et al.* Comparison of HERG channel blocking effects of various beta-blockers—implication for clinical strategy. *Br J Pharmacol* 2006;**147**:642-652.
39. Lopez-Sendon J, Swedberg K, McMurray J, Tamargo J, Maggioni AP, Dargie H *et al.* Expert consensus document on beta-adrenergic receptor blockers. *Eur Heart J* 2004;**25**:1341-1362.
40. Neil-Dwyer G, Bartlett J, McAinsh J, Cruickshank JM. Beta-adrenoceptor blockers and the blood-brain barrier. *Br J Clin Pharmacol* 1981;**11**: 549-553.
41. Leenen FH. Brain mechanisms contributing to sympathetic hyperactivity and heart failure. *Circ Res* 2007;**101**:221-223.
42. Gourine A, Bondar SI, Spyer KM, Gourine AV. Beneficial effect of the central nervous system beta-adrenoceptor blockade on the failing heart. *Circ Res* 2008;**102**:633-636.

Biochemical and Biophysical Research Communications 378 (2009) 851–856

Contents lists available at ScienceDirect

Biochemical and Biophysical Research Communications

journal homepage: www.elsevier.com/locate/ybbrc

Knockout of the *l-pgds* gene aggravates obesity and atherosclerosis in mice

Reiko Tanaka [a,b], Yoshikazu Miwa [a,*], Kin Mou [a], Morimasa Tomikawa [c], Naomi Eguchi [d], Yoshihiro Urade [d], Fumi Takahashi-Yanaga [a], Sachio Morimoto [a], Norio Wake [b], Toshiyuki Sasaguri [a]

[a] *Department of Clinical Pharmacology, Faculty of Medical Sciences, Kyushu University, 3-1-1, Maidashi, Higashi-ku, Fukuoka 812-8582, Japan*
[b] *Department of Obstetrics and Gynecology, Faculty of Medical Sciences, Kyushu University, Fukuoka, Japan*
[c] *Department of Future Medicine and Innovative Medical Information, Faculty of Medical Sciences, Kyushu University, Fukuoka, Japan*
[d] *Department of Molecular Behavioral Biology, Osaka Bioscience Institute, Suita, Japan*

ARTICLE INFO

Article history:
Received 26 November 2008
Available online 12 December 2008

Keywords:
Lipocalin-type prostaglandin D synthase
Apolipoprotein E
Knockout mice
Atherosclerosis
Interleukin-1β
Monocyte chemoattractant protein type-1
Obesity

ABSTRACT

This study was designed to determine whether *lipocalin type-prostaglandin D synthase* (*l-pgds*) deficiency contributes to atherogenesis using gene knockout (KO) mice. A high-fat diet was given to 8-week-old C57BL/6 (wild type; WT), *l-pgds* KO (LKO), *apolipoprotein E* (*apo E*) KO (AKO) and *l-pgds*/*apo E* double KO (DKO) mice. The *l-pgds* deficient mice showed significantly increased body weight, which was accompanied by increased size of subcutaneous and visceral fat tissues. Fat deposition in the aortic wall induced by the high-fat diet was significantly increased in LKO mice compared with WT mice, although there was no significant difference between AKO and DKO mice. In LKO mice, atherosclerotic plaque in the aortic root was also increased and, furthermore, macrophage cellularity and the expression of pro-inflammatory cytokines such as interleukin-1β and monocyte chemoattractant protein-1 were significant increased. In conclusion, *l-pgds* deficiency induces obesity and facilitates atherosclerosis, probably through the regulation of inflammatory responses.

Lipocalin-type prostaglandin D synthase (L-PGDS) is the enzyme that converts PGH_2 into PGD_2 in the process of an arachidonic acid metabolism. The synthesized PGD_2 is further non-enzymatically metabolized to the PGJ_2 series including PGJ_2, Δ^{12}-PGJ_2 and 15-deoxy-$\Delta^{12,14}$-PGJ_2 (15d-PGJ_2) [1]. Because L-PGDS is highly expressed in the central nervous system, its role in neurological disorders has been well studied [2–4]. In addition, recent studies have revealed that L-PGDS is constitutively expressed in the vascular endothelium [5] and that the downstream PGs, PGD_2 and the PGJ_2 series mainly act as protective factors for blood vessels [6]. The role of 15d-PGJ_2 has received particular attention because it was reported as a natural ligand of the nuclear receptor peroxisome proliferator-activated receptor-γ (PPARγ) that induces the differentiation of adipose cells and macrophages [7,8], which contribute to insulin resistance. 15d-PGJ_2 has been shown to be a unique material that is able to protect the vessel wall from injurious stimuli by controlling cell fate such as proliferation, differentiation and apoptosis, and by inhibiting inflammation in the vascular wall [6,9,10].

L-PGDS is secreted into the blood and urine, and several clinical studies have suggested a close association between L-PGDS levels and cardiovascular disease or its risk factors. The urinary L-PGDS level is significantly increased in patients with hypertension [11]. The L-PGDS concentration is increased in both serum and urine in diabetic patients and blood sugar control reversed the increase in urinary excretion of L-PGDS [12]. We previously reported that the serum L-PGDS level increases with aging and is associated with subclinical atherosclerosis as evaluated by the maximal intima–media complex thickness of the common carotid artery (C-IMT *max*) and by the pulse wave velocity [13]. In addition, we have identified single nucleotide polymorphisms (SNPs) in the *l-pgds* gene in Japanese people, and showed that a common SNP 4111A>C influences C-IMT *max* [14]. These observations strongly suggest the importance of L-PGDS in the pathogenesis of atherosclerosis; however, its role in vivo has not been well investigated.

Therefore, in the present study, to clarify the pathophysiologic role of L-PGDS in atherosclerosis, we investigated the effects of a high-fat diet on atherosclerosis and related parameters in *l-pgds* gene knockout (LKO) mice. We also crossed these mice with *apolipoprotein E (apo E)* knockout (AKO) mice, which are frequently used as a model of atherosclerosis, to generate a double knockout (DKO), and similarly investigated this phenotype.

Methods

Animals. All animal experiments were approved by the Committee on the Ethics of Animal Experiments, Kyushu University Graduate School of Medical Sciences. LKO mice were generated as previously described [4]. AKO mice and C57BL/6 (wild type, WT)

* Corresponding author. Fax: +81 92 642 6084.
E-mail address: ymiwa@clipharm.med.kyushu-u.ac.jp (Y. Miwa).

0006-291X/$ - see front matter © 2008 Elsevier Inc. All rights reserved.
doi:10.1016/j.bbrc.2008.11.152